Goodness-of-fit Measures Based on the Mellin Transform for Beta Generalized Lifetime Data

J. M. Vasconcelos[a], R. J. Cintra[b,c] and A. D. C. Nascimento[b]

[a]Departamento de Estatística e Informática, Universidade Federal Rural de Pernambuco, Recife, PE, Brazil; [b]Departamento de Estatística, Universidade Federal de Pernambuco, Recife, PE, Brazil; [c] ECE, University of Calgary, AB, Canada

ARTICLE HISTORY
Compiled March 29, 2021

Acknowledgments

We would like to acknowledge the partial financial support from CNPq and from CAPES - Finance code 001.

ABSTRACT
In recent years various probability models have been proposed for describing lifetime data. Increasing model flexibility is often sought as a means to better describe asymmetric and heavy tail distributions. Such extensions were pioneered by the beta-G family. However, efficient goodness-of-fit (GoF) measures for the beta-G distributions are sought. In this paper, we combine probability weighted moments (PWMs) and the Mellin transform (MT) in order to furnish new qualitative and quantitative GoF tools for model selection within the beta-G class. We derive PWMs for the Fréchet and Kumaraswamy distributions; and we provide expressions for the MT, and for the log-cumulants (LC) of the beta-Weibull, beta-Fréchet, beta-Kumaraswamy, and beta-log-logistic distributions. Subsequently, we construct LC diagrams and, based on the Hotelling's T^2 statistic, we derive confidence ellipses for the LCs. Finally, the proposed GoF measures are applied on five real data sets in order to demonstrate their applicability.

KEYWORDS
Class beta-G; Mellin transform; second-kind statistic; probability weighted moments; Hotelling's T^2 statistic

1. Introduction

Survival analysis tools have been applied in several contexts, such as survival time of mechanical components [1], the failure times of electrical insulator films [2], the effect of varying IL-2 concentration on T cell response [3], and in censored data from head-and-neck-cancer clinical trials [4]. Further applications were found in digital image processing, for instance in synthetic aperture radar (SAR) imagery analysis [5,6]. The derivation of new probability models capable of better explaining reliability data is

CONTACT J. M. Vasconcelos. E-mail: josimar.vasconcelos@ufrpe.br

a central task in the field of survival analysis. In recent years, an effort to extend classical models by means of probability distribution generators has been sought [7]. As a result, the following probability models were introduced: the Marshall and Olking (MG)-G class of distributions [8], the generalized exponential distribution [9], the beta-normal distribution [7], the Kumaraswamy (Kw)-G class [10], the McDonald normal distribution [11], the generalized gamma distribution [12,13], the T-X family of distributions [14,15], and the generalized Weibull distribution [16].

Despite the significant number of new models, few goodness-of-fit (GoF) measures have been proposed for the recent distributions; thus hindering model selection. Considering progressive type-II censored data, Pakyari and Balakrishnan [17] proposed a general GoF test [18] that encompasses the GoF test described in [19]. Such methods are based on distance measures between theoretical and empirical cumulative distribution functions.

Taking a different approach, Linhart and Zucchini [20] proposed information-theoretical measures considering the Akaike and Bayesian information criteria [21] as figures of merit for model selection. An alternative method for GoF assessment was given by the Pearson system diagram for model selection [22], which is based on skewness and kurtosis measures [23, p. 23]. Delignon *et al.* [24] and Vogel and Fennessey [25] applied such diagram for SAR and hydrology data, respectively. Chabert and Tourneret [26] introduced a generalization of the Pearson diagram for bivariate random vectors. Nagahara [27] examined the problem of devising GoF measures for multivariate non-normal distributions by using the Pearson system.

However, in [28], Nicolas noticed that the Pearson diagram tends not to be well-suited for positive random variables. Thus, the log-cumulant (LC) diagram, which plots the third-kind LC $\widetilde{\kappa}_3$ against the second-kind LC $\widetilde{\kappa}_2$, was introduced as an alternative [28]. The LC diagram offers some advantages over the Pearson diagram. Besides being suitable for positive random variables, its computational implementation is more direct and it also captures the distribution flexibility in the sense of skewness and kurtosis [29]. Such diagram was demonstrated to be relevant for quantitative and qualitative comparison of non-nested distributions in SAR and Polarimetric SAR (PolSAR) data [30–33]. A detailed description of the LC diagram is provided in [28,29]. In [28], Nicolas proposed the application of the Mellin transform (MT) [34, p. 50] as an alternative to the usual characteristic function. Li *et al.* [29] also considered the MT-based diagram for the classification of empirical probability density functions (pdf) from SAR imagery data. Nicolas and Maruani [35] compared the MT-based method with the second kind cumulant, moment, lower order moment, and maximum likelihood (ML) methods. Khan and Guida [32] have applied the MT to describe complex vector data having the $\mathcal{G}$ model; whereas Anfinsen and Eltoft [36] have demonstrated that MT can be useful for PolSAR data analysis.

In this paper, we propose a combination of probability weighted moments (PWMs) and the MT in order to furnish new GoF qualitative and quantitative tools for model selection in classes of generalized distributions [7]. We introduce a general expression for the MT of the beta generalized (beta-G) distributions. Because of analytical tractability and suitability for beta-generalization, we separate the following baseline distributions for investigation: Weibull [37], Fréchet [38,39], Kumaraswamy [40], and log-logistic (LL) [41]. Their corresponding beta-generalizations are: the beta-Weibull (BW) [42], the beta-Fréchet (BF) [43], the beta-Kumaraswamy (BKw) [44], and the beta-LL (BLL) [45] distributions. We introduce closed-form expressions for the Fréchet and Kumaraswamy PWM functions. Moreover, we propose a relationship between the Hotelling's T^2 statistic and the multivariate delta method to obtain asymptotic confidence ellipses for hypothesis testing that involves second kind cumulants. Based on Monte Carlo experiments, the performance of the proposed GoF tests are quantified e compared with that due to other well-defined tests. Finally, five actual data sets in the context of survival analysis were submitted to the proposed methodology.

The structure of this work is outlined as follows. Section 2 reviews the beta-G class of distributions with four particular cases. In Section 3, the MT and its properties are outlined. Moreover, we summarize the PWM theory and derive the PWM for the Fréchet and Kw distributions. Section 4 presents new GoF measures for four extended models from the beta-G class. In Section 5, numerical results are displayed. Finally, concluding remarks are presented in Section 6.

2. The Beta-G Distribution Family

The beta-G family of distributions was proposed by Eugene *et al.* [7] and is defined as follows. Let $G(x;\boldsymbol{\tau})$ be a cumulative distribution function (cdf) with parameter vector $\boldsymbol{\tau}$. We refer to such cdf as the baseline distribution. The beta-G approach extends the baseline distribution into another distribution $F(x)$ according to:

$$F(x) = F(x;a,b,\boldsymbol{\tau}) = I_{G(x;\boldsymbol{\tau})}(a,b)\frac{1}{B(a,b)}\int_0^{G(x;\boldsymbol{\tau})} \omega^{a-1}(1-\omega)^{b-1}\,\mathrm{d}\,\omega, \qquad (1)$$

where $a>0$ and $b>0$ are shape parameters, $I_y(a,b) = B_y(a,b)/B(a,b)$ is the incomplete beta function ratio, $B_y(a,b) = \int_0^y \omega^{a-1}(1-\omega)^{b-1}\ \mathrm{d}\,\omega$ is the incomplete beta function, $B(a,b) = \Gamma(a)\Gamma(b)/\Gamma(a+b)$ is the beta function, and $\Gamma(a) = \int_0^\infty \omega^{a-1}\,\mathrm{e}^{-\omega}\,\mathrm{d}\,\omega$ is the gamma function. The pdf associated with (1) is given by:

$$f(x) = f(x;a,b,\boldsymbol{\tau}) = \frac{1}{B(a,b)}\,g(x;\boldsymbol{\tau})G(x;\boldsymbol{\tau})^{a-1}[1-G(x;\boldsymbol{\tau})]^{b-1}, \qquad (2)$$

where $g(x;\boldsymbol{\tau}) = \mathrm{d}\,G(x;\boldsymbol{\tau})/\,\mathrm{d}\,x$ is the baseline pdf. In the next subsections, we separate four particular beta-G distribution, given in Table 1, for further assessment and derivation of GoF measures.

Figure 1 presents pdf curves of BW, BF, BKw, and BLL for several parameters values. Due to the inclusion of shape parameters (a and b), these distributions are more flexible than their baselines and are candidates for modeling positive real data sets [46–48].

3. Mellin Transform as a Special PWM: Second Kind Statistics for Beta Generalized Models

The Fourier transform is a central tool in signal analysis [49,50]. Traditionally a probability distribution can be described by means of its characteristic function (cf) of the first kind, which is the Fourier transform of its pdf. Let X be random variable equipped with cdf $F(x)$. Then, its cf $\Phi_X(t)$ is defined as [51, p. 342]:

$$\Phi_X(t) = \mathrm{E}(\mathrm{e}^{\mathrm{i}\,t\,X}) = \int_{-\infty}^{\infty} \mathrm{e}^{\mathrm{i}\,t\,x}\ \mathrm{d}\,F(x), \quad t\in\mathbb{R},$$

where $\mathrm{i} = \sqrt{-1}$. However, the cf can be not analytically tractable, as noticed in the BW [42], BF [43], BKw [44], BLL [45], beta-Gumbel [43], and beta log-normal [52] models. To address this issue, Colombo [53] has suggested the MT as an alternative. In [28], Nicolas introduced the second kind statistics based on the MT for analyzing distributions over $\mathbb{R}_+$.

In this section, we show that the MT of beta-G distributions can be directly obtained from the PWM of baseline distributions. For such, in the following, we review PWM for baseline distributions.

3.1. PWM Background

PWM was introduced by Greenwood *et al.* [54] and consists of a generalized moment expression for probability models. In terms of estimation theory, PWMs can furnish useful closed-form estimators when classical estimators, such as the method of moments and ML, are analytically intractable [54–56].

The PWM is defined by

$$\mathcal{M}_{l,j,k} = \mathrm{E}\left\{X^l F(X)^j [1-F(X)]^k\right\} = \int_0^1 Q[F(x)]^l F(x)^j (1-F(x))^k \, \mathrm{d}\, F(x), \tag{3}$$

where $l, j, k \in \mathbb{R}$ and $Q(\cdot)$ represents the quantile function of $F(\cdot)$. Notice that (3) generalizes the usual moments, which are obtained by taking $l \in \mathbb{Z}_+$ and $j = k = 0$ ($\mathcal{M}_{l,0,0}$). If $\mathcal{M}_{l,0,0}$ is finite, then PWM $\mathcal{M}_{l,j,k}$ is well-defined for all $j, k \in \mathbb{R}_+$ [54]. Table 2 presents the quantile function, the cdf, and the sample space $\mathcal{X}$ for the baseline distributions considered in this paper.

3.2. PWM of Particular Baseline Distributions

Greenwood *et al.* [54] and Caiza and Ummenhofer [57] derived the PWM for the following models: the Weibull, the Gumbel [54], the generalized lambda [54], the logistic [54,57], the Wakeby [54], and the kappa distribution [54]. Mahdi and Ashkar [58] derived the PWM for the LL model as a means to investigate the generalized probability weighted moments and ML fitting methods. They also showed how to provide an estimation based on PWMs. Mahdi and Ashkar [59,60] also derived and described PWMs linked to the Weibull and LL models as an alternative to estimation methods such as the generalized PWMs [61], generalized moments [62–64], and ML methods [65].

However, the current literature lacks PWM expressions for the Fréchet and Kw distributions. In the following propositions, we address this literature gap.

Proposition 3.1. *Let X be a random variable following the Fréchet model with $\lambda > 0$ and $\alpha > 0$ as location and shape parameters, respectively. The PWM of X is given by*

$$\mathcal{M}_{l,j,k} = \lambda^l \Gamma\left(1 - \frac{l}{\alpha}\right) \sum_{r=0}^{\infty} \binom{k}{r} (-1)^r \frac{1}{(j+r+1)^{1-\frac{l}{\alpha}}}.$$

Proposition 3.2. *Let X be a random variable following the Kw model with shape* *parameters $\lambda > 0$ and $\alpha > 0$. The PWM of X is given by*

$$\mathcal{M}_{l,j,k} = \lambda \sum_{r=0}^{\infty} \binom{j}{r} (-1)^r \, B\left[1 + \frac{l}{\alpha}, \, \lambda(k + r + 1)\right].$$

Proofs for the above propositions are given in the Appendix A. A summary of the PWM results is listed in Table 3; central moments are also shown as particular cases.

3.3. Mellin Transform

Let $X \in \mathbb{R}_+$ be a random variable with cdf $F(x)$. Then the first cf of the second kind is defined by means of the MT:

$$\phi_X(s) = \int_0^\infty x^{s-1} \, \mathrm{d}\, F(x) = \mathrm{E}(X^{s-1}), \tag{4}$$

where $s \in \mathbb{C}$ is a complex variable [28].

Considering the beta-G family, we introduce the following theorem relating the MT to the PWMs.

Theorem 3.3. *Let X be a random variable having distribution in the beta-G family with cdf and pdf given by (1) and (2), respectively. Then, the MT of X, referred to as $\phi_{BG}(s)$, is given by*

$$\phi_{BG}(s) = \frac{1}{B(a,\, b)} \mathcal{M}_{s-1,\, a-1,\, b-1}, \tag{5}$$

where $\mathcal{M}_{s-1,\, a-1,\, b-1}$ is the PWM of a baseline G.

Proof. Applying (1) into (4) with $\overline{G}(x) = 1 - G(x)$ we can show that:

$$\begin{aligned}
\phi_{\mathrm{BG}}(s) &= \int_0^\infty x^{s-1} \;\, \mathrm{d}\, F(x) \\
&= \int_0^\infty x^{s-1} \, \frac{g(x)}{B(a,\, b)} \, G(x)^{a-1} \overline{G}(x)^{b-1} \;\, \mathrm{d}\, x \\
&= \frac{1}{B(a,\, b)} \int_0^\infty x^{s-1} \, G(x)^{a-1} \overline{G}(x)^{b-1} \;\, \mathrm{d}\, G(x) \\
&= \frac{1}{B(a,\, b)} \, \mathrm{E}\left[X^{\, s-1} \; G(X)^{a-1} \overline{G}(X)^{b-1}\right] \\
&= \frac{1}{B(a,\, b)} \, \mathcal{M}_{s-1,\, a-1,\, b-1}.
\end{aligned}$$

□

Table 4 displays the obtained MT for the considered distributions.

The second cf of the second kind is defined as follows:

$$\psi_X(s) = \log\left(\phi_X(s)\right). \tag{6}$$

The second kind cumulants or LCs of order ν are obtained from the νth derivative of $\psi_X(s)$ evaluated at $s = 1$:

$$\widetilde{\kappa}_\nu = \left.\frac{\mathrm{d}^\nu\, \psi_X(s)}{\mathrm{d}\, s^\nu}\right|_{s=1}, \qquad \nu \in \mathbb{N}. \tag{7}$$

Table 5 presents LCs for the considered beta-G models.

3.4. The Log-cumulants Diagram

As discussed by Delignon *et al.* [24], the Pearson diagram is a tool for model selection and assessment of fitting. Such diagram is based on skewness and kurtosis measures. Nicolas [28] presented evidence that the Pearson diagram can be analytically intractable and introduced the $(\widetilde{\kappa}_3, \widetilde{\kappa}_2)$ diagram, which is similar to the Pearson diagram, but employs the second kind statistics $\widetilde{\kappa}_3$ and $\widetilde{\kappa}_2$ instead of skewness and kurtosis measures. In [28], it is also shown that the $(\widetilde{\kappa}_3, \widetilde{\kappa}_2)$ diagram is a suitable alternative for classifying SAR images whose associate Pearson diagram is often intractable.

Anfinsen and Eltoft [30] introduced the matrix LC (MLC) diagram as means to visually inspect the multidimensional space where each dimension is represented by one particular MLC with order ν. Thus, such visualization tool facilitates the use of MT and provides intuition to the LC method. The diagram in [30] is an extension of the LC diagram considered by Nicolas [28,66] for the univariate MT. In [29,31,32,36], the MT-based LC diagram was employed for pdf classification from SAR imagery data.

In this paper, we employ the $(\widetilde{\kappa}_3, \widetilde{\kappa}_2)$ diagram as a tool for assessing fits under beta-G models. The LCs (see Table 5) of such models were derived using PWMs and the MT and are displayed in Table 5, where the LCs are given in terms of the digamma and polygamma functions given by $\psi(z) = \frac{\mathrm{d}}{\mathrm{d}\, z} \log \Gamma(z)$ and $\psi^{(n)}(z) = \frac{\mathrm{d}^{n+1}}{\mathrm{d}\, z^{n+1}} \log \Gamma(z)$ [67, p. 258–260], respectively.

Figure 2 exhibits the regions in the $(\widetilde{\kappa}_3, \widetilde{\kappa}_2)$ diagram linked to the BW, BF, BKw, and BLL models. These regions can be understood as manifolds [30]. Each distribution is represented by a subspace, whose dimensions depend on the parameter number of the associated distribution [30,36]. However, the resulting region can degenerate into a curve [30,36]. For instance, the LL distribution has no shape parameters and its manifold is represented by a line (vertical dashed line), which can be viewed as a zero-dimensional manifold.

The regions linked to the BW and BF distributions are parameterized by one parameter. These regions are represented, respectively, by a solid and dotted curve in Figure 2 of the Diagram of the LCs $(\widetilde{\kappa}_3, \widetilde{\kappa}_2)$ for BW, BF, BKw, and BLL models, being one-dimensional manifolds. On the other hand, the BKw and BLL distributions result in two-dimensional manifold because they are parametrized by two and three parameters, respectively.

4. New GoF Tools for Beta-G Models

In recent years, several models have been proposed to describe survival data, such as the beta power exponential [68], McDonald exponentiated gamma [69], gamma extended Weibull [70], and the models considered in this paper. These models are however in need of accurate GoF tools. In this section, we propose four GoF tools for beta-G models based on the Hotelling's T^2 statistic [71, p. 170].

4.1. Hotelling's $\boldsymbol{T^2}$ Statistic

The Hotelling's T^2 statistic is a generalization of the Student's t statistics [71, p. 170] given by:

$$T^2 = n\left(\overline{\boldsymbol{x}} - \boldsymbol{\mu}\right)^\top \boldsymbol{S}^{-1}\left(\overline{\boldsymbol{x}} - \boldsymbol{\mu}\right), \tag{8}$$

where $\overline{\boldsymbol{x}} = \frac{1}{n}\sum_{r=1}^{n} \boldsymbol{x}_r$ is the sample mean vector based on a random sample $\boldsymbol{x}_1, \boldsymbol{x}_2, \ldots, \boldsymbol{x}_n$ from the ν-variate normal random vector $\boldsymbol{x} \sim \mathcal{N}_\nu(\boldsymbol{\mu}, \boldsymbol{\Sigma})$; $\boldsymbol{\mu}$ and $\boldsymbol{\Sigma}$ are the mean vector and covariance matrix, respectively; and $\boldsymbol{S} = \frac{1}{n}\sum_{r=1}^{n} \boldsymbol{x}_r \boldsymbol{x}_r^\top - n\overline{\boldsymbol{x}}\,\overline{\boldsymbol{x}}^\top$ is the sample covariance matrix. Such statistics follows the F-Snedecor distribution with ν and $n-\nu$ degrees of freedom denoted by $F_{\nu,n-\nu}$ [71, p. 177].

Considering a significance level η, the likelihood ratio test for the hypothesis $\mathrm{E}(\overline{\boldsymbol{X}}) = \boldsymbol{\mu}$ can be rejected if $T^2 \geq Q_F(1-\eta; \nu, n-\nu)$, where $Q_F(\cdot; \nu, n-\nu)$ is the quantile function for $F_{\nu,n-\nu}$ [71]. Additionally one may consider ν-dimensional confidence ellipsoids given by [71]:

$$n\left(\overline{\boldsymbol{x}} - \boldsymbol{\mu}\right)^\top \boldsymbol{S}^{-1}\left(\overline{\boldsymbol{x}} - \boldsymbol{\mu}\right) \leq Q_F(1-\eta; \nu, n-\nu).$$

For large samples, the T^2 distribution can be approximated by its limiting distribution, which is the chi-squared distribution with ν degrees of freedom [36]. This result is relevant for the case where $\boldsymbol{x}_r$ is not normal and the exact distribution for (8) is not known.

4.2. Hotelling's $\boldsymbol{T^2}$ statistic and Log-cumulants

We aim at applying the Hotelling's T^2 statistic as a means for proposing GoF tests based on the LCs. Our goal is to estimate the LCs and then classify the underlying distribution according to the location of the estimated LCs $\begin{bmatrix}\widehat{\widetilde{\kappa}}_2 & \widehat{\widetilde{\kappa}}_3\end{bmatrix}^\top$ over the $(\widetilde{\kappa}_3, \widetilde{\kappa}_2)$ diagram.

Therefore, we need a test statistics for the null hypothesis $\mathcal{H}_0 : \mathrm{E}\left(\begin{bmatrix}\widehat{\widetilde{\kappa}}_2 & \widehat{\widetilde{\kappa}}_3\end{bmatrix}\right) = \begin{bmatrix}\widetilde{\kappa}_2 & \widetilde{\kappa}_3\end{bmatrix}$. Such test would pave the way for accepting or rejecting the pertinence of estimated LCs to particular regions over the $(\widetilde{\kappa}_3, \widetilde{\kappa}_2)$ diagram.

Because the LCs tend to be analytically well-defined quantities, they can be given closed-form expressions, as we showed in Table 5, for several beta-G distributions. Such relationship between parameters and LCs can be used to derive estimators for the LCs. In other words, we have that

$$\widehat{\widetilde{\kappa}}_2 = g_2(\widehat{\boldsymbol{\theta}}) \quad \text{and} \quad \widehat{\widetilde{\kappa}}_3 = g_3(\widehat{\boldsymbol{\theta}}),$$

where $\widehat{\boldsymbol{\theta}}$ is the estimated parameter vector; and $g_2(\cdot)$ and $g_3(\cdot)$ are composite functions that return the LCs in terms of the baseline distribution parameters by means of evaluating: (7), (6), (4), and (5).

Further, we notice that for large samples, considering the generalized delta method [72], the estimator vector $\begin{bmatrix}\widehat{\widetilde{\kappa}}_2 & \widehat{\widetilde{\kappa}}_3\end{bmatrix}^\top$ follows the bivariate normal distribution with mean $\begin{bmatrix}\widetilde{\kappa}_2 & \widetilde{\kappa}_3\end{bmatrix}^\top$ and an asymptotic covariance matrix $\boldsymbol{K}$, as previously shown in [31,32,36]. The estimated asymptotic covariance matrix $\widehat{\boldsymbol{K}}$ can be obtained from the asymptotic covariance matrix of the parameter estimators $\mathbf{\Sigma}$ [36]. As shown in [36, p. 2769], we can write

$$\widehat{\boldsymbol{K}} = \widehat{\boldsymbol{J}}^\top \cdot \widehat{\mathbf{\Sigma}} \cdot \widehat{\boldsymbol{J}},$$

where

$$\widehat{\boldsymbol{J}} = \begin{bmatrix} \frac{\partial g_2(\widehat{\boldsymbol{\theta}})}{\partial \widehat{\theta}_1} & \frac{\partial g_3(\widehat{\boldsymbol{\theta}})}{\partial \widehat{\theta}_1} \\ \frac{\partial g_2(\widehat{\boldsymbol{\theta}})}{\partial \widehat{\theta}_2} & \frac{\partial g_3(\widehat{\boldsymbol{\theta}})}{\partial \widehat{\theta}_2} \\ \vdots & \vdots \\ \frac{\partial g_2(\widehat{\boldsymbol{\theta}})}{\partial \widehat{\theta}_r} & \frac{\partial g_3(\widehat{\boldsymbol{\theta}})}{\partial \widehat{\theta}_r} \end{bmatrix}, \tag{9}$$

θ_r is the rth parameter of the model and $\widehat{\mathbf{\Sigma}}$ is the estimated asymptotic covariance matrix of the estimator vector $\widehat{\boldsymbol{\theta}}$.

The ML estimators for the parameters of beta-G distributions often have no closed-form expressions and its covariance matrix is unknown. This is illustrated by the beta-Pareto [47], beta-Laplace [73], BW [42], and BF [74] distributions.

As presented in [65, p. 181–182] and [75,76], the inverse of Fisher information matrix (FIM) can be employed as an approximation for the variance-covariance matrix, since it is the asymptotic covariance matrix of the ML estimators [65, p. 181–182]. Thus, we have the following approximation for $\mathbf{\Sigma}$ [77, Th. 7.3.11]:

$$\mathbf{\Sigma} \approx -\left[\mathrm{E}\left(\frac{\partial^2 \ell(\boldsymbol{\theta})}{\partial \boldsymbol{\theta}^\top \partial \boldsymbol{\theta}}\right)\right]^{-1}, \tag{10}$$

under regularity conditions [65].

For the majority of beta-G models, the calculation of their FIMs is analytically intractable. A common solution for this problem is the use of the observed information matrix instead of the FIM, as supported by [47,73,78]. Thus, the observed information matrix is an estimator for the FIM [79]. Therefore, in this work, we use the inverse observed information matrix as replacement for the asymptotic covariance matrix of the ML estimators. The observed information matrix has the advantage of being definite positive matrix; thus measuring the observed curvature on the log-likelihood surface. In other words, it provides an indication of how much a multidimensional likelihood surface is rotated with respect to the parameter axes [80]. For the model parameter estimation, we employed the ML estimation because it results in invariant, consistent, and asymptotically efficient estimators [81, p. 3].

Thus, comparing with (8) and (9), for second and third order LCs $\widetilde{\kappa}_2$ and $\widetilde{\kappa}_3$, we have that $\nu = 2$, $\boldsymbol{\mu} = \begin{bmatrix}\widetilde{\kappa}_2 & \widetilde{\kappa}_3\end{bmatrix}^\top$, $\overline{\boldsymbol{x}} = \begin{bmatrix}\widehat{\widetilde{\kappa}}_2 & \widehat{\widetilde{\kappa}}_3\end{bmatrix}^\top$, where $\widehat{\widetilde{\kappa}}_2$ and $\widehat{\widetilde{\kappa}}_3$ are sample estimators for $\widetilde{\kappa}_2$ and $\widetilde{\kappa}_3$, respectively. The matrix $\mathbf{S}$ can be substituted by the estimated asymptotic covariance matrix $\widehat{\boldsymbol{K}}$ of $[\widehat{\widetilde{\kappa}}_2, \widehat{\widetilde{\kappa}}_3]^\top$. Therefore, we obtain the following statistic:

$$T^2 = n\left(\begin{bmatrix}\widehat{\widetilde{\kappa}}_2 \\ \widehat{\widetilde{\kappa}}_3\end{bmatrix} - \begin{bmatrix}\widetilde{\kappa}_2 \\ \widetilde{\kappa}_3\end{bmatrix}\right)^\top \widehat{\boldsymbol{K}}^{-1}\left(\begin{bmatrix}\widehat{\widetilde{\kappa}}_2 \\ \widehat{\widetilde{\kappa}}_3\end{bmatrix} - \begin{bmatrix}\widetilde{\kappa}_2 \\ \widetilde{\kappa}_3\end{bmatrix}\right), \tag{11}$$

where the inverse of $\widehat{\boldsymbol{K}}$ is obtained via usual matrix inversion [82,83] if the matrix $\widehat{\boldsymbol{K}}$ is nonsingular [84, p. 508]; otherwise the generalized Moore-Penrose inverse [84,85] is applied.

For such, we submit the estimated LCs $\widehat{\widetilde{\kappa}}_2$ and $\widehat{\widetilde{\kappa}}_3$ from the $(\widetilde{\kappa}_3, \widetilde{\kappa}_2)$ diagram [28] to the Hotelling's T^2 statistic formalism. Considering large samples, the limiting distribution of the random variable T^2 is the χ^2 distribution [36]. Thus, in (11), we can adopt the approximation $Q_F(\cdot;\nu, n-\nu) \approx Q_{\chi^2}(\cdot;\nu)$, where $Q_{\chi^2}(\cdot;\nu)$ is the quantile function for the χ^2 distribution with ν degrees of freedom. Therefore, we can derive a confidence ellipse at significance level η according to:

$$\left(\begin{bmatrix}\widehat{\widetilde{\kappa}}_2\\ \widehat{\widetilde{\kappa}}_3\end{bmatrix} - \begin{bmatrix}\widetilde{\kappa}_2\\ \widetilde{\kappa}_3\end{bmatrix}\right)^\top \widehat{\boldsymbol{K}}^{-1} \left(\begin{bmatrix}\widehat{\widetilde{\kappa}}_2\\ \widehat{\widetilde{\kappa}}_3\end{bmatrix} - \begin{bmatrix}\widetilde{\kappa}_2\\ \widetilde{\kappa}_3\end{bmatrix}\right) \leq \frac{1}{n} Q_{\chi^2}(\eta;2),$$

where $Q_{\chi^2}(\eta;2)$ is the quantile function for χ^2_2. The above ellipse is centered at $(\widetilde{\kappa}_2, \widetilde{\kappa}_3)$ and its axes are directed according the eigenvectors of $\widehat{\boldsymbol{K}}$ [86].

4.3. Hotelling's T^2 statistic for Selected Beta-G Distributions

Based on the last discussion, four GoF measures are proposed for the BW, BF, BKw, and BLL distributions.

Proposition 4.1. *Let X be a random variable following the BW distribution with parameters $a = 1$, $b > 0$, $\alpha > 0$ and $\lambda > 0$, then the Hotelling's T^2 statistic, here referred to as T^2_{BW}, based on the LCs is given by*

$$T^2_{BW} = \frac{n\widehat{\alpha}^6}{4}\left(\frac{1}{\widehat{\alpha}^2} - \frac{1}{\alpha^2}\right)^2 \left(\frac{|\widehat{\boldsymbol{H}}_{BW}|}{U_{\widehat{\alpha}\widehat{\alpha}} U_{\widehat{b}\widehat{b}} - U^2_{\widehat{\lambda}\widehat{b}}}\right),$$

where $|\cdot|$ is the determinant of a matrix $\widehat{\boldsymbol{H}}.$; $|\widehat{\boldsymbol{H}}_{BW}|$ is the estimator of $|\boldsymbol{H}_{BW}|$ given by

$$|\boldsymbol{H}_{BW}| = U_{\alpha\alpha}(U_{\lambda\lambda}U_{bb} - U^2_{\lambda b}) + U_{\alpha\lambda}(U_{\alpha b}U_{\lambda b} - U_{\alpha\lambda}U_{bb}) + U_{\alpha b}(U_{\alpha\lambda}U_{\lambda b} - U_{\alpha b}U_{\lambda\lambda});$$

and $\widehat{\alpha}$, $\widehat{b}$, $\widehat{\lambda}$ are the estimators for α, b, and λ, respectively. The quantities $U.$ are the entries of the associated information matrix and are given in the Appendix B.

Proposition 4.2. *Let X be a random variable following the BF distribution with parameters $a > 0$, $b = 1$, $\lambda > 0$ and $\alpha > 0$, then the Hotelling's T^2 statistic, referred to as T^2_{BF}, based on the LCs is given by*

$$T^2_{BF} = \frac{n\widehat{\alpha}^6}{4}\left(\frac{1}{\widehat{\alpha}^2} - \frac{1}{\alpha^2}\right)^2 \left(\frac{|\widehat{\boldsymbol{H}}_{BF}|}{U_{\widehat{\alpha}\widehat{\alpha}} U_{\widehat{a}\widehat{a}} - U^2_{\widehat{\lambda}\widehat{a}}}\right),$$

where $|\widehat{\boldsymbol{H}}_{BF}|$ is the estimator of $|\boldsymbol{H}_{BF}|$ given by

$$|\boldsymbol{H}_{BF}| = U_{\alpha\alpha}(U_{\lambda\lambda}U_{aa} - U^2_{\lambda a}) + U_{\alpha\lambda}(U_{\alpha a}U_{\lambda a} - U_{\alpha\lambda}U_{aa}) + U_{\alpha a}(U_{\alpha\lambda}U_{\lambda a} - U_{\alpha a}U_{\lambda\lambda});$$

and $\widehat{\alpha}$, $\widehat{a}$, $\widehat{\lambda}$ are the estimates of the α, a, and λ, respectively. In the Appendix B, the *quantities U. are fully detailed.*

Proposition 4.3. *Let X be a random variable following the BKw with parameters $a = 1$, $b > 0$, $\lambda > 0$ and $\alpha > 0$, then its Hotelling's T^2 statistic, here called T^2_{BKw}, is given by*

$$T^2_{BKw} = \frac{n|\widehat{\boldsymbol{H}}_{BKw}|}{\widehat{\delta}_{22}\widehat{\delta}_{33} - \widehat{\delta}^2_{23}} \cdot \left[\widehat{\delta}_{33}\left(\widehat{\widetilde{\kappa}}_2 - \widetilde{\kappa}_2\right)^2 + \widehat{\delta}_{22}\left(\widehat{\widetilde{\kappa}}_3 - \widetilde{\kappa}_3\right)^2 - 2\widehat{\delta}_{23}\left(\widehat{\widetilde{\kappa}}_2 - \widetilde{\kappa}_2\right)\left(\widehat{\widetilde{\kappa}}_3 - \widetilde{\kappa}_3\right)\right],$$

where $|\widehat{\boldsymbol{H}}_{BKw}|$ is an estimator of $|\boldsymbol{H}_{BKw}|$ is given by

$$|\boldsymbol{H}_{BKw}| = U_{\alpha\alpha}(U_{\lambda\lambda}U_{bb} - U^2_{\lambda b}) + U_{\alpha\lambda}(U_{\alpha b}U_{\lambda b} - U_{\alpha\lambda}U_{bb}) + U_{\alpha b}(U_{\alpha\lambda}U_{\lambda b} - U_{\alpha b}U_{\lambda\lambda});$$

and $\widehat{\widetilde{\kappa}}_2$ and $\widehat{\widetilde{\kappa}}_3$ are the estimates of the LCs $\widetilde{\kappa}_2$ and $\widetilde{\kappa}_3$, respectively; and $\widehat{\delta}_{22}$, $\widehat{\delta}_{23}$, and $\widehat{\delta}_{33}$ are the estimates for δ_{22}, δ_{23}, and δ_{33} given in compact form by

$$\begin{aligned}
\delta_{22} &= \begin{bmatrix} J_{12} & J_{22} & J_{32} \end{bmatrix} \cdot \boldsymbol{\Sigma}_{BKw} \cdot \begin{bmatrix} J_{12} & J_{22} & J_{32} \end{bmatrix}^\top, \\
\delta_{23} &= \begin{bmatrix} J_{12} & J_{22} & J_{32} \end{bmatrix} \cdot \boldsymbol{\Sigma}_{BKw} \cdot \begin{bmatrix} J_{13} & J_{23} & J_{33} \end{bmatrix}^\top, \\
\delta_{33} &= \begin{bmatrix} J_{13} & J_{23} & J_{33} \end{bmatrix} \cdot \boldsymbol{\Sigma}_{BKw} \cdot \begin{bmatrix} J_{13} & J_{23} & J_{33} \end{bmatrix}^\top;
\end{aligned}$$

and

$$\begin{aligned}
J_{12} &= \frac{2}{\alpha^3}\left\{\psi^{(1)}(\lambda b + 1) - \psi^{(1)}(1)\right\}, \\
J_{13} &= \frac{3}{\alpha^4}\left\{\psi^{(2)}(\lambda b + 1) - \psi^{(2)}(1)\right\}, \\
J_{22} &= \frac{b}{\alpha^2}\psi^{(2)}(\lambda b + 1), \quad J_{23} = \frac{b}{\alpha^3}\psi^{(3)}(\lambda b + 1), \\
J_{32} &= \frac{\lambda}{\alpha^2}\psi^{(2)}(\lambda b + 1), \quad J_{33} = \frac{\lambda}{\alpha^3}\psi^{(3)}(\lambda b + 1).
\end{aligned}$$

For the sake of brevity, the matrix $\boldsymbol{\Sigma}_{BKw}$ is shown in Appendix B.4 where the above expressions are also given fully expanded forms.

Proposition 4.4. *Let X be a random variable following the BLL distribution with parameters $a > 0$, $b = 1$, $\lambda > 0$ and $\alpha > 0$, then its Hotelling's T^2 statistic, here named T^2_{BLL}, based on the LCs is given by*

$$T^2_{BLL} = \frac{n|\boldsymbol{H}_{BLL}|}{\widehat{\delta}_{22}\widehat{\delta}_{33} - \widehat{\delta}^2_{23}} \left[\widehat{\delta}_{33}\left(\widehat{\widetilde{\kappa}}_2 - \widetilde{\kappa}_2\right)^2 + \widehat{\delta}_{22}\left(\widehat{\widetilde{\kappa}}_3 - \widetilde{\kappa}_3\right)^2 - 2\widehat{\delta}_{23}\left(\widehat{\widetilde{\kappa}}_2 - \widetilde{\kappa}_2\right)\left(\widehat{\widetilde{\kappa}}_3 - \widetilde{\kappa}_3\right)\right],$$

where $|\widehat{\boldsymbol{H}}_{BLL}|$ is an estimator of $|\boldsymbol{H}_{BLL}|$ is given by

$$|\boldsymbol{H}_{BLL}| = U_{\alpha\alpha}(U_{\lambda\lambda}U_{aa} - U^2_{\lambda a}) + U_{\alpha\lambda}(U_{\alpha a}U_{\lambda a} - U_{\alpha\lambda}U_{aa}) + U_{\alpha a}(U_{\alpha\lambda}U_{\lambda a} - U_{\alpha a}U_{\lambda\lambda});$$

and $\widehat{\widetilde{\kappa}}_2$ and $\widehat{\widetilde{\kappa}}_3$ are the estimates of the LCs $\widetilde{\kappa}_2$ and $\widetilde{\kappa}_3$, respectively; $\widehat{\delta}_{22}$, $\widehat{\delta}_{23}$, and $\widehat{\delta}_{33}$

are the estimates for δ_{22}, δ_{23}, and δ_{33} given in compact form by

$$\begin{aligned}
\delta_{22} &= \begin{bmatrix}0 & J_{22} & J_{32}\end{bmatrix} \cdot \mathbf{\Sigma}_{BLL} \cdot \begin{bmatrix}0 & J_{22} & J_{32}\end{bmatrix}^\top, \\
\delta_{23} &= \begin{bmatrix}0 & J_{22} & J_{32}\end{bmatrix} \cdot \mathbf{\Sigma}_{BLL} \cdot \begin{bmatrix}0 & J_{23} & J_{33}\end{bmatrix}^\top, \\
\delta_{33} &= \begin{bmatrix}0 & J_{23} & J_{33}\end{bmatrix} \cdot \mathbf{\Sigma}_{BLL} \cdot \begin{bmatrix}0 & J_{23} & J_{33}\end{bmatrix}^\top;
\end{aligned}$$

and

$$\begin{aligned}
J_{22} &= -\frac{2}{\lambda^3}\left\{\psi^{(1)}(a) + \psi^{(1)}(1)\right\}, \\
J_{23} &= -\frac{3}{\lambda^4}\left\{\psi^{(2)}(a) - \psi^{(2)}(1)\right\}, \\
J_{32} &= \frac{1}{\lambda^2}\psi^{(2)}(a), \quad J_{33} = \frac{1}{\lambda^3}\psi^{(3)}(a).
\end{aligned}$$

The matrix $\mathbf{\Sigma}_{BLL}$ is shown in Appendix B.5 with the above expressions fully expanded.

4.4. Mellin-based GoF tests

It is known a GoF test consists at testing as null hypothesis ($\mathcal{H}_0$) whereas a set of random variables follows a specific distribution. For a totally specified distribution, when all its parameters are known, $\mathcal{H}_0$ is said to be a simple hypothesis. When any of the parameters are unknown, the null hypothesis is composite and the associated problem is of composite GoF [87]. According to D' Agostino and Stephens [88], to derive a GoF test, different ways are adopted. The most manners are: Pearson's χ^2 test, tests based on the EDF (Empirical Distribution Function) and tests based on moments. The classic Anderson–Darling, and Cramér–von Mises tests are qualified as EDF-based tests. Moment-based strategies to GoF problems have been introduced in [89] and [90].

In Algorithm (1), we displayed a contextual summary of the Monte Carlo simulation for the general case of the evaluation of the test statistics given in Propositions 4.1–4.4. In next section, following Algorithm (1), we will illustrate the effectiveness of the Hotellings T^2 statistics for the BW, BF, BKW and BLL models, comparing with the Anderson–Darling and Cramér–von Mises statistics for some scenarios.

5. Simulations study and Application to Actual Data

5.1. Simulations Study

The Mellin-based GoF test has been recently developed for PolSAR distributions [36]. Now we are in position to check the performance of the GoF tests given in (11) resulting from Propositions 4.1–4.4.

To that end, we do a Monte Carlo simulation with five thousand replicas and, for each replica, samples drawn from the BW($\boldsymbol{\theta}_1$), BF($\boldsymbol{\theta}_2$), BKW($\boldsymbol{\theta}_3$) and BLL($\boldsymbol{\theta}_4$) distributions are generated. As parametric setting, we use $\boldsymbol{\theta}_1 \in \{(1,1,5,1),\ (1,1,8,1)\}$, $\boldsymbol{\theta}_2 \in \{(1,1,8,1),\ (1,1,3,2)\}$, $\boldsymbol{\theta}_3 \in \{(1,1,0.5,8),\ (1,1,1,15)\}$ and $\boldsymbol{\theta}_4 \in \{(1,1,8,0.6), (1,1,8,1)\}$. Further, we use the nominal levels $\eta \in \{1\%, 5\%, 10\%\}$ and sample sizes

Algorithm 1: LC-based GoF test of the composite hypothesis with Monte Carlo simulation of the test statistic sampling distribution

Step 1. Determine the significance level η;

Step 2. Generate a sample of size n from a probability distribution (BW, BF, BKw or BLL);

Step 3. Estimate the parameters of $\boldsymbol{\theta}$ of the hypothesized from distribution model and determine the LCs this model;

Step 4. Generate the observed information matrix of the hypothesized from distribution model;

Step 5. Use the obtained sample in **Step 2** to compute the required sample LCs by means of the moment-to-cumulant transformations;

Step 6. Obtained the Hotelling's T^2 statistics given in Propositions 4.1–4.4, here called T_{p}^2;

Step 7. Randomly generate m samples of size n under the hypothesized model. For each sample, repeat **Steps 2-6** and store the simulated test statistics as $\{T_s^2(i)\}_{i=1}^m$.

Step 8. Count the number of simulated test statistics that are larger than the test statistic T_{p}^2 obtained in **Step 6** and compute the fraction with respect to the number of Monte Carlo simulations. This yields the p value, this is,

$$P_{\mathrm{MC}} = \frac{1}{m}\sum_{i=1}^{m} \mathbb{I}\big(T_{\mathrm{s}}^2(i) > T_{\mathrm{p}}^2\big),$$

where $\mathbb{I}(\cdot)$ is the indicator function subjecte to the superscripted condition. That is, we compute the fraction of simulated $T_{\mathrm{s}}^2(i)$ that are larger than T_{p}^2. The Monte Carlo simulated p value P_{MC} is then evaluated against the chosen significance level η in the test rejected $\mathcal{H}_0$ if $P_{\mathrm{MC}} < \eta$.

Step 9. Perform the hypothesis test by comparing the p value to the significance level.

$n \in \{10, 15, 20, 100\}$. The performance of the proposed GoF tools is compared with those due to the Arderson-Darling (AD) and Cramer-von Mises (W) tests [19].

Table 6 displays the empirical test sizes. Results show that the proposed GoF tests outperform the others. See for example the scenario for BW model, with $\eta = 1\%$ and $\boldsymbol{\theta} = (1, 1, 5, 1)$.

5.2. Selected Data Sets and Descriptive Statistics

We separated five real data sets to be submitted to our proposed methodology, determining according to the introduced GoF criteria a suitable candidate among the BW, BF, BKw, and BLL models. In the following, we describe briefly the selected data sets:

(i) Breaking (BR) data [91]: 100 observations on breaking stress of carbon fibres (in Gba);
(ii) Guinea.pig (GU) data [92]: 72 survival times of guinea pigs injected with different doses of tubercle bacilli;
(iii) Stress-rupture (SR) data [93]: the stress-rupture life of kevlar 49/epoxy strands subjected to constant sustained pressure at the 90% stress level until failure;
(iv) Airborne (AI) data [94,95]: repair times (in hours) for an airborne communication transceiver;
(v) River flow (RF) data [96]: lower discharge of at least seven consecutive days and return period (time) of ten years ($Q_{7,10}$) of the Cuiabá River, Mato Grosso, Brazil.

Table 7 gives the descriptive summary for each data set. The first and second data sets are homogeneous with sample variation coefficient (VC) of 38.68% and 37.26%, respectively. The remaining data sets are heterogeneous. The river flow data set has negative skeweness and platykurtic distribution (kurtosis is less than 3). The remaining data sets have positive skeweness with leptokurtic distribution (kurtosis is greater than 3).

5.3. $(\widetilde{\kappa}_3, \widetilde{\kappa}_2)$ Diagram and Log-cumulants Estimation

Figure 4 exhibits the $(\widetilde{\kappa}_3, \widetilde{\kappa}_2)$ diagram and regions linked to particular distributions are emphasized. For each data set, we computed the sample LCs according to bootstrap sampling with 1,000 replicates and 90% sample sizes. Each data set is represented by a different dot pattern.

For each data set, we computed the 95% confidence interval in each replications (sample sizes $n \in \{10, 50, 100, 300\}$) and repeated this process 1,000 times to compute these intervals without the Bonferroni correction (WOBC) and with the Bonferroni correction (WBC). Bellow Table 8 displays centers and ranges of the confidence interval for bootstrap percentile WOBC and WBC. We note that for the five data sets the larger the sample size the smaller confidence interval. Both for the WOBC and WBC methods. Also, we highlight that for all data sets and in all scenarios ($n \in \{10, 50, 100, 300\}$ and the second and third order sample LCs), the method WOBC had a lower confidence interval that WBC.

Qualitatively we have the following analysis. For the breaking stress and stress-rupture data sets, most of the points are located over the regions linked to the BKw and BW distributions. The points derived from the Guinea.pig data are located in the BLL distribution region. The airborne data set has its associated points over the central region, which includes the LL distribution region, and over the BLL and BF distribution regions. Finally, we have the river flow data set, where the BKw distribution region captures most of its points, while some of them spread over the BW and LL distribution regions.

5.4. Hotelling's T^2 statistic Analysis

The Hotelling's T^2 statistic with p values were computed and are displayed in bellow table 9. The obtained statistics can be interpreted as a measure of the distance between the data and each particular beta-G model. Lower values of Hotelling's T^2 statistic suggest a better agreement between data and model; indicating therefore a better data fitting.

By separating the models linked to the smallest values of Hotelling's T^2 statistic, we have that the BLL distribution is a good model for the guinea.pig and airborne data sets. The stress-rupture and breaking data could be better modeled by the BW distribution. Similarly, the river flow data could be fitted under the BKw distribution. These quantitative results confirm the qualitative analysis provided in Figure 4.

5.5. Confidence Ellipses

To complement the previous analysis of visual application, we have plotted confidence ellipses for each data set. The construction of the ellipses was based on (11). We employed the smallest value of Hotelling's T^2 statistic from Table 9 and the associated beta-G distribution using the estimated LCs $\widehat{\widetilde{\kappa}}_2$ and $\widehat{\widetilde{\kappa}}_3$; and the sample variance-covariance matrix $\widehat{\Sigma}$.

To obtain the ellipse for breaking and stress-rupture data set we used the BW model with the T^2_{BW} statistics given by Proposition 4.1. For the guinea.pig and airborne data set we apply the BLL model with the T^2_{BLL} statistics given by Proposition 4.4. In the case of the river flow data, we apply the BKw model with the T^2_{BKw} statistics given by Proposition 4.3. Figure 5 depicts the obtained ellipses.

6. Conclusion

In this paper, several GoF measures have been proposed for determining good fits at the beta-G class in the survival analysis context. We provided qualitative and quantitative analyses for the introduced GoF tools including numerical and visual inspection approaches. We derived closed-form expressions for the second kind characteristic function, LCs, Hotelling's T^2 statistic, and ellipse of confidence for the LCs of the BW, BF, BKw, and BLL distributions. Further, Monte Carlo experiments have been made to assess the performance of the GoF tests proposed to some beta-G models. Proposed measures have been applied to five real data sets in order to demonstrate their applicability.

References

[1] Nascimento ADC, Bourguignon M, Zea LM, et al. The gamma extended Weibull family of distributions. Journal of Statistical Theory and Applications. 2014;13:1–16.

[2] Alizadeh M, Cordeiro GM, Nascimento ADC, et al. Odd-Burr generalized family of distributions with some applications. Journal of Statistical Computation and Simulation. 2016;87:367–389.
[3] Deenick EK, Gett AV, Hodgkin PD. Stochastic model of T cell proliferation: A calculus revealing IL-2 regulation of precursor frequencies, cell cycle time, and survival. The Journal of Immunology. 2003;170:4963–4972.
[4] Lee C, Famoye F, Olumolade O. Beta-Weibull distribution: some properties and applications to censored data. Journal of Modern Applied Statistical Methods. 2007;6:173–186.
[5] Cintra RJ, Frery AC, Nascimento ADC. Parametric and nonparametric tests for speckled imagery. Pattern Analysis and Applications. 2013;16:141–161.
[6] Cintra RJ, Rêgo LC, Cordeiro GM, et al. Beta generalized normal distribution with an application for SAR image processing. A Journal of Theoretical and Applied Statistics. 2012;48:279–294.
[7] Eugene N, Lee C, Famoye F. Beta-normal distribution and its applications. Communications in Statistics - Theory and Methods. 2002;31:497–512.
[8] Marshall AW, Olkin I. A new method for adding a parameter to a family of distributions with application to the exponential and Weibull families. Biometrika. 1997;84:641–652.
[9] Gupta RD, Kundu D. Generalized exponential distributions. Australian & New Zealand Journal of Statistics. 1999;41:173–188.
[10] Cordeiro GM, de Castro M. A new family of generalized distributions. Journal of Statistical Computation and Simulation. 2010;87:1–16.
[11] Cordeiro GM, Cintra RJ, Rêgo LC, et al. The McDonald normal distribution. Pakistan Journal of Statistics and Operation Research. 2012;8:301–329.
[12] Ristic MM, Balakrishnan N. The gamma exponentiated exponential distribution. Journal of Statistical Computation and Simulation. 2012;82:1191–1206.
[13] Zografos K, Balakrishnan N. On families of beta- and generalized gamma-generated distributions and associated inference. Statistical Methodology. 2009;6:344–362.
[14] Aljarrah MA, Lee C, Famoye F. On generating T-X family of distributions using quantile functions. Journal of Statistical Distributions and Applications. 2014;1:1–17.
[15] Alzaatreh A, Lee C, Famoye F. A new method for generating families of continuous distributions. METRON. 2013;71:63–79.
[16] Cordeiro GM, Ortega EMM, Ramire TG. A new generalized Weibull family of distributions: mathematical properties and applications. Journal of Statistical Distributions and Applications. 2015;2:1–25.
[17] Pakyari R, Balakrishnan N. A general purpose approximate goodness-of-fit test for progressively type-II censored data. IEEE transactions on reliability. 2012;61:238–244.
[18] Viveros R, Balakrishnan N. Interval estimation of parameters of life from progressively censored data. Technometrics. 1994;36:84–91.
[19] Chen G, Balakrishnan N. A general purpose approximate good-ness-of-fit test. Journal of Quality Technology. 1995;27:154–161.
[20] Linhart H, Zucchini W. Model selection. John Wiley & Sons; 1986.
[21] McQuarrie ADR, Tsai CL. Regression and time series model selection. World Scientific; 1998.
[22] Pearson K. Memoir on skew variation in homogeneous material. Philosophical Transactions of the Royal Society of London A: Mathematical, Physical and Engineering Sciences. 1895;:343–414.
[23] Johnson NL, Kotz S, Balakrishnan N. Continuous univariate distributions. 2nd ed. Vol. 1. Wiley; 1994.
[24] Delignon Y, Garello R, Hillion A. Statistical modelling of ocean SAR images. IEE Proceedings-Radar. 1997;144:348–354.
[25] Vogel RM, Fennessey NM. L moment diagrams should replace product moment distribution. Water resources research. 1993;29:1745–1752.
[26] Chabert M, Tourneret JY. Bivariate Pearson distributions for remote sensing imagens. IEEE International Geoscience and Remote Sensing Symposium. 2011;:4038–4041.

[27] Nagahara Y. A method of simulating multivariate nonnormal distributions by the Pearson distribution system and estimation. Computational Statistics & Data Analysis. 2004;47:1–29.
[28] Nicolas JM. Introduction aux statistiques de deuxième espèce: applications des logs-moments et des logs-cumulants à l'analyse des lois d'images radar. Traitement du Signal. 2002;19:139–167.
[29] Li HC, Hong W, Wu YR, et al. On the empirical-statistical modeling of SAR images with generalized gamma distribution. IEEE Journal of Selected Topics in Signal Processing. 2011;5:386–397.
[30] Anfinsen SN, Eltof T. Application of the matrix-variate Mellin transform to analysis of polarimetric radar images. IEEE Transactions on Geoscience and Remote Sensing. 2011; 49:2281–2295.
[31] Deng X, López-Martínez C. Higher order statistics for texture analysis and physical interpretation of polarimetric SAR data. IEEE Geoscience and Remote Sensing Letters. 2016; 13:912–916.
[32] Khan S, Guida R. Application of Mellin kind statistics to polarimetric G distribution for SAR data. IEEE Transactions on Geoscience and Remote Sensing. 2013;52:3513–3528.
[33] Krylov V, Moser G, Serpico SB, et al. On the method of logarithmic cumulants for parametric probability density function estimation. IEEE Signal Processing Society. 2013; 22:3791–3806.
[34] Johnson NL, Kemp AW, Kotz S. Univariate discrete distributions. 3rd ed. Wiley-Interscience; 2005.
[35] Nicolas JM, Maruani A. Lower order statistics: a new approach for probability density functions defined on $\mathbb{R}_+$. In: IEEE Signal Processing Conference; 2000. p. 1–4.
[36] Anfinsen SN, Doulgeris AP, Eltoft T. Goodness-of-fit tests for multilook polarimetric radar data based on the Mellin transform. IEEE Transactions on Geoscience and Remote Sensing. 2011;49:2764–2781.
[37] Weibull W. A statistical theory of the strength of material. The Royal Swedish Royal Institute for Engineering Research; 1939.
[38] Fréchet M. Sur la loi de probabilité de l'écart maximum. Annales de la Société Polonaise de Mathématique. 1927;6:30–38.
[39] Khan MS, PASHA GR, PASHA AH. Theoretical analysis of inverse Weibull distribution. WSEAS Transactions on Mathematics. 2008;7:93–116.
[40] Kumaraswamy P. Generalized probability density-function for double-bounded random-processes. Journal of Hydrology. 1980;46:79–88.
[41] Shah BK, Dave PH. A note on log-logistic distribution. Journal of the MS University of Baroda. 1963;12:15–20.
[42] Famoye F, Lee C, Olumolade O. The beta-Weibull distribution. Journal Statistics Theory Application. 2005;4:121–136.
[43] Nadarajah S, Kotz S. The beta Gumbel distribution. Mathematical Problems in Engineering. 2004;4:323–332.
[44] Carrasco JMF, Ferrari SLP, Cordeiro GM. A new generalized Kumaraswamy distribution. 2010;.
[45] Lemonte AJ. The beta log-logistic distribution. Brazilian Journal of Probability and Statistics. 2014;28:313–332.
[46] Achcar JA, Coelho-Barros EA, Cordeiro GM. Beta generalized distributions and related exponentiated models: A bayesian approach. Brazilian Journal of Probability and Statistics. 2013;27:1–19.
[47] Akinsete A, Famoye F, Lee C. The beta-Pareto distribution. Statistics. 2008;42:547–563.
[48] Cordeiro GM. A simple formula based on quantiles for the moments of beta generalized distributions. Journal of Statistical Computation and Simulation. 2013;83:1932–1943.
[49] Averbuch A, RRCoifman, Donoho D, et al. Fast and accurate polar Fourier transform. Applied and Computational Harmonic Analysis. 2006;21:145–167.
[50] Oppenheim AV, Schafer RW. Discrete-time signal processing. Upper Saddle River, NJ,

USA: Prentice Hall Press; 2009.
[51] Bilingsley P. Probability and measure. 4th ed. Wiley; 2016.
[52] Castellares F, Montenegro LC, Cordeiro GM. The beta log-normal distribution. Journal of Statistical Computation and Simulation. 2013;83:203–228.
[53] Colombo S. Les transformations de Mellin et de Hankel: applications à la physique mathématique. Centre National de la Recerche Scientifique; 1959.
[54] Greenwood JA, Landwehr JM, Matalas NC, et al. Probability weighted moments: definition and relation to parameters of several distributions expressable in inverse form. Water Resources. 1979;15:1049–1054.
[55] Haktanir T, Bozduman A. A study on sensitivity of the probability-weighted moments method on the choice of the plotting position formula. Journal of Hydrology. 1995;168:265–281.
[56] Whalen TM, Savage GT, Jeong GD. An evaluation of the self-determined probability-weighted moment method for estimating extreme wind speeds. Journal of Wind Engineering and Industrial Aerodynamics. 2004;92:219–239.
[57] Caiza PDT, Ummenhofer T. General probability weighted moments for the three-parameter Weibull distribution and their application in S-N curves modelling. International Journal of Fatigue. 2011;1:1533–1538.
[58] Ashkar F, Mahdi S. Comparison of two fitting methods for the log-logistic distribution. Water Resources Research. 2003;39:1–8.
[59] Ashkar F, Mahdi S. Fitting the log-logistic distribution by generalized moments. Journal of Hydrology. 2006;328:694–703.
[60] Mahdi S, Ashkar F. Exploring generalized probability weighted moments, generalized moments and maximum likelihood estimating methods in two-parameter Weibull model. Journal of Hydrology. 2004;285:62–75.
[61] Rasmussen PF. Generalized probability weighted moments: Application to the generalized pareto distribution. Water Resources Research. 2001;37:1745–1751.
[62] Ashkar F, Bobée B. The generalized method of moments as applied to problems of flood frequency analysis: Some practical results for the log-Pearson type 3 distribution. Journal of Hydrology. 1987;90:199–217.
[63] Bobée B, Ashkar F. The generalized method of moments applied to the LP3 distribution. Journal of Hydraulic Engineering. 1988;114:899–909.
[64] Bobée B, Ashkar F. The gamma family and derived distributions applied in hydrology. Water Resources Publications; 1991.
[65] Bickel PJ, Doksum KA. Mathematical statistics: Basic ideas and selected topics. 2nd ed. Prentice–Hall; 2001.
[66] Nicolas JM. Application de la transformée de Mellin: Étude des lois statistiques de l'imagerie cohérente. Paris, France: Ecole Nationale Supérieure des Télécommunications; 2017.
[67] Abramowitz M, Stegun IA. Handbook of mathematical functions with formulas, graphs, and mathematical tables. Dover; 1964.
[68] Adepoju KA, Chukwu AU, Wang M. The beta power exponential distribution. Journal of Statistical Science and Application. 2014;2:37–46.
[69] Al-Babtain AA, Merovci F, Elbatal I. The McDonald exponentiated gamma distribution and its statistical properties. Springer. 2015;4:1–22.
[70] Cordeiro GM, do C S Lima M, Gomes AE, et al. The gamma extended Weibull distribution. Journal of Statistical Distributions and Applications. 2016;3:1–19.
[71] Anderson TW. An introduction to multivariate statistical analysis. Wiley; 2003. Wiley series in probability and statistics.
[72] Lehmann EL, Casella G. Theory of point estimation. 2nd ed. Vol. 1. Springer; 1998.
[73] Cordeiro GM, Lemonte AJ. The beta Laplace distribution. Statistics and Probability Letters. 2011;81:973–982.
[74] Nadarajah S, Gupta AK. The beta Fréchet distribution. Far East Journal of Theoretical Statistics. 2004;14:15–24.

[75] Anfinsen SN, Doulgeris AP, Eltoft T. Estimation of the equivalent number of looks in polarimetric synthetic aperture radar imagery. IEEE Transactions on Geoscience and Remote Sensing. 2009;47:3795–3809.
[76] Bustos OH, Lucini MM, Frery AC. M-Estimators of roughness and scale for GA0-modelled SAR imagery. EURASIP Journal on Applied Signal Processing. 2002;1:105–114.
[77] Casella G, Berger RL. Statistical inference. 2nd ed. Duxbury Press; 2002.
[78] Cordeiro GM, Silva GO, Ortega EMM. The beta-Weibull geometric distribution. Statistics. 2013;47:817–834.
[79] Cordeiro GM, Lemonte AJ. The β-Birnbaum-Saunders distribution: An improved distribution for fatigue life modeling. Computational Statistics and Data Analysis. 2011; 1:1445–1461.
[80] Lindsey JK. Parametric statistical inference. Oxford Science Publications; 1996.
[81] Cordeiro GM, Cribari-Neto F. An introduction to Bartlett correction and bias reduction. SpringerBriefs in Statistics; 2014.
[82] Harville DA. Matrix algebra from a statistician's perspective. Springer; 1997.
[83] Rencher AC, Schaalje GB. Linear models in statistics. 2nd ed. John Wiley & Sons; 2008.
[84] C R Rao SCH H Toutenburg, Schomaker M. Linear models and generalizations: Least squares and alternatives. Springer; 2008.
[85] Seber GAF. A matrix handbook for statisticians. 1st ed. New York, NY, USA: Wiley-Interscience; 2007.
[86] Härdle WK, Simar L. Applied multivariate statistical analysis. Springer; 2007.
[87] DasGupta A. Asymptotic theory of statistics and probability. Springer New York; 2008. Springer Texts in Statistics.
[88] D'Agostino R. Goodness-of-fit-techniques. Taylor & Francis; 1986. Statistics: A Series of Textbooks and Monographs.
[89] Papadopoulos A, Li G. A note on goodness of fit test using moments. Statistica. 2007 Oct;62(1):71–86.
[90] Natarajan R, Mudholkar GS. Moment-based goodness-of-fit tests for the inverse gaussian distribution. Technometrics. 2004;46(3):339–347. Available from: https://doi.org/10.1198/004017004000000365.
[91] Nichols MD, Padgett WJ. A bootstrap control chart for Weibull percentiles. Quality and Reliability Engineering International. 2006;22:141–151.
[92] G M Cordeiro RRP, Ortega EMM. The Kumaraswamy generalized Half-normal distribution for skewed positive data. Journal of Data Science. 2012;10:195–224.
[93] Paranaiba PF, Ortega EMM, Cordeiro GM, et al. The Kumaraswamy Burr XII distribution: theory and practice. Journal of Wind Engineering and Industrial Aerodynamics. 2013;83:2117–2143.
[94] Alven WHV. Reliability engineering by arinc. ; 1964.
[95] Jø rgensen B. Statistical properties of the generalized inverse gaussian distribution. (Lecture Notes in Statistics; Vol. 9). ; 1982.
[96] Cordeiro GM, Nadarajah S, Ortega EMM. The Kumaraswamy Gumbel distribution. Statistical Methods and Applications. 2012;21:139–168.
[97] Cordeiro GM, Silva GO, Pescim RR, et al. General properties for the beta extended Half-normal model. Journal of Statistical Computation and Simulation. 2014;84:881–901.
[98] Barreto-Souza W, Santos AHS, Cordeiro GM. The beta generalized exponential distribution. Journal of Statistical Computation and Simulation. 2010;80:159–172.
[99] Prudnikov AP, Brychkov YA, Marichev OI. Integrals and series: Special functions. Vol. 1. Taylor & Francis; 1986.

Table 1. Probability density function of the selected beta-G distributions

Models	$f(x)$	Reference
Beta-Weibul (BW)	$\frac{1}{B(a,b)}\frac{\alpha}{x}\left(\frac{x}{\lambda}\right)^{\alpha}\mathrm{e}^{-b\left(\frac{x}{\lambda}\right)^{\alpha}}\left[1-\mathrm{e}^{-\left(\frac{x}{\lambda}\right)^{\alpha}}\right]^{a-1}$	[13,42]
Beta-Fréchet (BF)	$\frac{1}{B(a,b)}\frac{\alpha}{x}\left(\frac{x}{\lambda}\right)^{-\alpha}\mathrm{e}^{-a\left(\frac{x}{\lambda}\right)^{-\alpha}}\left[1-\mathrm{e}^{-\left(\frac{x}{\lambda}\right)^{-\alpha}}\right]^{b-1}$	[43]
Beta-Kumaraswamy (BKw)	$\frac{\alpha\lambda\, x^{\alpha-1}}{B(a,b)}\left(1-x^{\alpha}\right)^{\lambda\, b-1}\left[1-\left(1-x^{\alpha}\right)^{\lambda}\right]^{a-1}$	[44]
Beta-log-logistic (BLL)	$\frac{(\lambda/\alpha)}{B(a,b)}\left(\frac{x}{\alpha}\right)^{\alpha\lambda-1}\left[1+\left(x/\alpha\right)^{\lambda}\right]^{-(a+b)}$	[45]

Table 2. Quantile and Cumulative Distribution of Adapted Baselines

Models	$Q[F(x)]$	$F(x)$	$\mathcal{X}$
Weibull	$\lambda\left[-\log(1-F(x))\right]^{1/\alpha}$	$1-\exp\left\{-\left(\frac{x}{\lambda}\right)^{\alpha}\right\}$	$\mathbb{R}_+$
Fréchet	$\lambda\left[-\log(F(x))\right]^{-1/\alpha}$	$\exp\left\{-\left(\frac{x}{\lambda}\right)^{-\alpha}\right\}$	$\mathbb{R}_+$
Kw	$\left[1-\left(1-F(x)\right)^{1/\lambda}\right]^{1/\alpha}$	$\left[1-\left(1-x^{\alpha}\right)^{\lambda}\right]$	$[0,\ 1]$
LL	$\alpha\left[\frac{F(x)}{1-F(x)}\right]^{1/\lambda}$	$\left[1+\left(\frac{\alpha}{x}\right)^{\lambda}\right]^{-1}$	$\mathbb{R}_+$

Table 3. Central Moments (CM) and Probability Weighted Moments

Models	PWM, $\mathcal{M}_{l,j,k}$	CM, $\mathcal{M}_{1,\,0,\,0}$	Restriction
Weibull	$\lambda^{l}\,\Gamma\left(1+\frac{l}{\alpha}\right)\sum_{r=0}^{\infty}\binom{j}{r}(-1)^{r}\frac{1}{(k+r+1)^{1+l/\alpha}}$	$\lambda\,\Gamma\left(1+\frac{1}{\alpha}\right)$	$l,k\in\mathbb{R},\ j\in\mathbb{R}_+$
Fréchet	$\lambda^{l}\,\Gamma\left(1-\frac{l}{\alpha}\right)\sum_{r=0}^{\infty}\binom{k}{r}(-1)^{r}\frac{1}{(j+r+1)^{1-l/\alpha}}$	$\lambda\,\Gamma\left(1-\frac{1}{\alpha}\right)$	$l,j\in\mathbb{R},\ k\in\mathbb{R}_+$
Kw	$\lambda\sum_{r=0}^{\infty}\binom{j}{r}(-1)^{r}\,B\left[1+l/\alpha,\ \lambda(k+r+1)\right]$	$\lambda\,B\left(1+1/\alpha,\ \lambda\right)$	$l>-\alpha$ and $k>-(r+1)$
LL	$\alpha^{l}\,B\left(j+l/\lambda+1,\ k-l/\lambda+1\right)$	$\alpha\,B\left(1+1/\lambda,\ 1-1/\lambda\right)$	$j>-(l/\lambda+1)$ and $k>l/\lambda-1$

Table 4. Mellin transform for the BW, BF, BKw, and BLL models

Models	MT	Restriction
BW	$\frac{\lambda^{s-1}}{B(1,b)}\,\Gamma\left(1+\frac{s-1}{\alpha}\right)b^{-(s\,-\,1\,+\,\alpha)/\alpha}$	for all $a=1, b>0, \alpha>0, \lambda>0$
BF	$\frac{\lambda^{s-1}}{B(a,1)}\,\Gamma\left(1-\frac{s-1}{\alpha}\right)a^{(s\,-\,1\,-\,\alpha)/\alpha}$	for all $b=1, a>0, \alpha>0, \lambda>0$
BKw	$\frac{\lambda}{B(1,b)}\,B\left(1+\frac{s-1}{\alpha},\,\lambda\,b\right)$	for all $a=1, b>0, \alpha>0, \lambda>0$
BLL	$\frac{\alpha^{s-1}}{B(a,1)}\,B\left(a+\frac{s-1}{\lambda},\,1-\frac{s-1}{\lambda}\right)$	for all $b=1, a>0, \alpha>0, \lambda>0$

Table 5. Log-cumulants of considered models

Model	$\widetilde{\kappa}_1$	$\widetilde{\kappa}_2$	$\widetilde{\kappa}_3$	$\cdots$	$\widetilde{\kappa}_\nu \quad \forall\,\nu>1$
BW	$\log(\lambda)+\frac{\psi(1)-\log(b)}{\alpha}$	$\frac{1}{\alpha^2}\psi^{(1)}(1)$	$\frac{1}{\alpha^3}\psi^{(2)}(1)$	$\cdots$	$\frac{1}{\alpha^\nu}\psi^{(\nu-1)}(1)$
BF	$\log(\lambda)-\frac{\psi(1)-\log(a)}{\alpha}$	$\frac{1}{\alpha^2}\psi^{(1)}(1)$	$-\frac{1}{\alpha^3}\psi^{(2)}(1)$	$\cdots$	$(-1)^\nu\frac{1}{\alpha^\nu}\psi^{(\nu-1)}(1)$
BKw	$\frac{\psi(1)-\psi(\lambda\,b+1)}{\alpha}$	$\frac{\psi^{(1)}(1)-\psi^{(1)}(\lambda\,b+1)}{\alpha^2}$	$\frac{\psi^{(2)}(1)-\psi^{(2)}(\lambda\,b+1)}{\alpha^3}$	$\cdots$	$\frac{\psi^{(\nu-1)}(1)-\psi^{(\nu-1)}(\lambda b+1)}{\alpha^\nu}$
BLL	$\log(\alpha)+\frac{\psi(a)-\psi(1)}{\lambda}$	$\frac{\psi^{(1)}(a)+\psi^{(1)}(1)}{\lambda^2}$	$\frac{\psi^{(2)}(a)-\psi^{(2)}(1)}{\lambda^3}$	$\cdots$	$\frac{\psi^{(\nu-1)}(a)+(-1)^\nu\ \psi^{(\nu-1)}(1)}{\lambda^\nu}$

Table 6. The GoF measure of the BW, BF, BKw, and BLL distribution, with $a = 1$ and $b = 1$ parameters.

Models	parameters	sample	1%			5%			10%		
			T^2	AD	CM	T^2	AD	W	T^2	AD	W
BW	$(\alpha = 5, \lambda = 1)$	10	99.94	98.44	99.54	99.54	92.22	97.56	99.12	92.30	94.06
		15	99.44	98.66	99.20	99.00	92.20	97.22	97.98	92.02	93.08
		20	99.26	98.22	99.02	98.12	92.62	97.02	97.88	91.88	93.30
		100	98.56	98.14	98.38	97.54	91.66	96.72	95.10	91.48	92.86
	$(\alpha = 8, \lambda = 1)$		99.92	97.80	99.40	99.70	89.90	95.98	99.30	89.12	90.70
			99.76	97.46	99.22	99.26	89.52	95.92	98.66	89.82	91.28
			99.54	97.76	99.30	98.90	89.16	95.16	98.32	89.36	91.28
			99.00	97.26	98.14	98.16	89.14	95.72	96.90	89.70	91.26
BF	$(\alpha = 8, \lambda = 1)$		100.00	97.82	99.28	100.00	89.84	95.88	100.00	90.42	92.40
			100.00	97.84	99.52	100.00	89.64	95.80	100.00	89.66	91.28
			99.98	97.16	99.12	99.96	89.04	95.42	99.42	89.04	91.14
			94.02	93.10	93.98	99.34	89.24	95.68	91.54	89.22	90.22
	$(\alpha = 3, \lambda = 2)$		99.86	99.38	99.84	99.88	95.76	98.82	97.56	95.50	96.00
			99.98	99.50	99.82	99.98	96.50	98.84	99.94	96.86	97.12
			99.96	99.38	99.82	99.94	96.52	98.72	99.98	96.02	96.48
			99.82	99.26	99.36	99.06	95.38	98.34	90.02	96.10	96.62
BKW	$(\alpha = 0.5, \lambda = 8)$		99.96	99.54	99.92	99.92	97.10	99.10	99.96	97.48	97.72
			99.90	99.56	99.88	99.96	96.64	98.72	99.90	97.06	97.16
			99.94	99.38	99.76	99.82	97.12	99.02	99.94	96.54	97.06
			100.00	99.28	99.86	99.98	95.72	98.68	100.00	95.60	96.18
	$(\alpha = 1, \lambda = 15)$		99.44	99.58	99.90	99.44	96.44	98.74	99.44	96.08	96.46
			99.88	99.56	99.86	99.86	97.36	98.86	99.88	97.36	97.34
			99.90	99.44	99.94	99.96	96.84	98.60	99.90	96.78	97.04
			100.00	99.46	99.80	100.00	96.22	98.48	100.00	96.26	96.46
BLL	$(\alpha = 8, \lambda = 0.6)$		79.26	31.04	46.98	79.42	18.02	29.72	77.08	18.34	22.20
			76.82	23.66	35.14	75.34	13.20	23.14	75.30	13.12	16.58
			86.62	19.58	30.08	81.52	18.80	18.58	82.02	19.74	13.50
			22.40	15.14	15.68	22.34	14.02	14.30	21.38	14.08	14.36
	$(\alpha = 8, \lambda = 1)$		74.26	38.68	50.60	73.54	28.06	37.82	73.54	27.66	30.78
			72.16	32.18	42.98	72.52	21.60	30.76	71.94	20.58	23.44
			78.46	26.16	38.80	78.32	16.48	25.04	78.38	15.30	18.18
			22.04	10.68	18.86	20.68	10.36	18.16	21.08	10.34	16.80

Table 7. Descriptive statistics and LCs ($\widehat{\widehat{\kappa}}_2$ and $\widehat{\widehat{\kappa}}_3$) for selected data sets

Data	Mean	Median	SD	Skewness	Kurtosis	VC (%)	$\widehat{\widehat{\kappa}}_2$	$\widehat{\widehat{\kappa}}_3$
BR	2.62	2.70	1.01	0.36	3.10	38.68	0.19	−0.09
GU	99.82	70.00	81.12	1.80	5.61	81.26	0.50	0.04
SR	1.02	0.80	1.12	3.00	16.71	109.22	2.02	−2.71
AI	3.64	1.75	5.07	2.91	11.67	139.34	1.18	0.35
RF	107.60	114.10	40.90	−0.15	1.93	37.26	0.19	−0.06

Table 8. Centers and ranges of the confidence interval for bootstrap percentile WOBC and WBC

Data	n	Center				Range			
		$\widehat{\widehat{\kappa}}_2$		$\widehat{\widehat{\kappa}}_3$		$\widehat{\widehat{\kappa}}_2$		$\widehat{\widehat{\kappa}}_3$	
		WOBC	WBC	WOBC	WBC	WOBC	WBC	WOBC	WBC
BR	10	0.254	0.270	−0.191	−0.224	0.395	0.454	0.417	0.508
	50	0.205	0.215	−0.111	−0.130	0.175	0.215	0.205	0.251
	100	0.200	0.206	−0.101	−0.107	0.129	0.153	0.162	0.182
	300	0.198	0.199	−0.089	−0.095	0.073	0.088	0.094	0.115
GU	10	0.487	0.526	0.001	−0.027	0.674	0.810	0.706	0.842
	50	0.505	0.504	0.029	0.027	0.335	0.398	0.306	0.379
	100	0.500	0.503	0.035	0.033	0.232	0.291	0.225	0.263
	300	0.502	0.503	0.041	0.041	0.134	0.166	0.131	0.153
SR	10	1.928	2.032	−2.850	−3.106	2.878	3.371	6.049	7.159
	50	2.016	2.015	−2.556	−2.643	1.395	1.693	2.927	3.440
	100	2.001	2.018	−2.661	−2.631	0.952	1.151	2.122	2.515
	300	2.020	2.018	−2.678	−2.675	0.547	0.648	1.183	1.476
AI	10	1.144	1.183	0.373	0.359	1.477	1.660	2.076	2.628
	50	1.175	1.172	0.372	0.378	0.697	0.773	1.080	1.280
	100	1.170	1.174	0.365	0.367	0.479	0.567	0.777	0.938
	300	1.168	1.173	0.355	0.358	0.271	0.320	0.450	0.521
RF	10	0.179	0.179	−0.057	−0.064	0.232	0.268	0.140	0.169
	50	0.186	0.186	−0.058	−0.058	0.111	0.126	0.070	0.080
	100	0.185	0.184	−0.058	−0.060	0.074	0.087	0.047	0.060
	300	0.185	0.185	−0.059	−0.059	0.045	0.053	0.027	0.033

Table 9. Hotelling's T^2 statistic and p-value (in parentheses) with respect to the data sets

Models	Breaking	Guinea.pig	Stress-rupture	Airborne	River flow
BW	0.178 (0.8367)	6.727 (0.0021)	0.055 (0.9462)	2.949 (0.0638)	2.681 (0.0821)
BF	>10 (≈ 0.00)	5.466 (0.0062)	>10 (≈ 0.00)	2.393 (0.1042)	2.289 (0.1159)
BKw	6.772 (0.0018)	>10 (≈ 0.00)	0.133 (0.8752)	>10 (≈ 0.00)	0.225 (0.7990)
BLL	5.500 (0.0054)	0.862 (0.4266)	>10 (≈ 0.00)	0.318 (0.7289)	0.935 (0.4016)

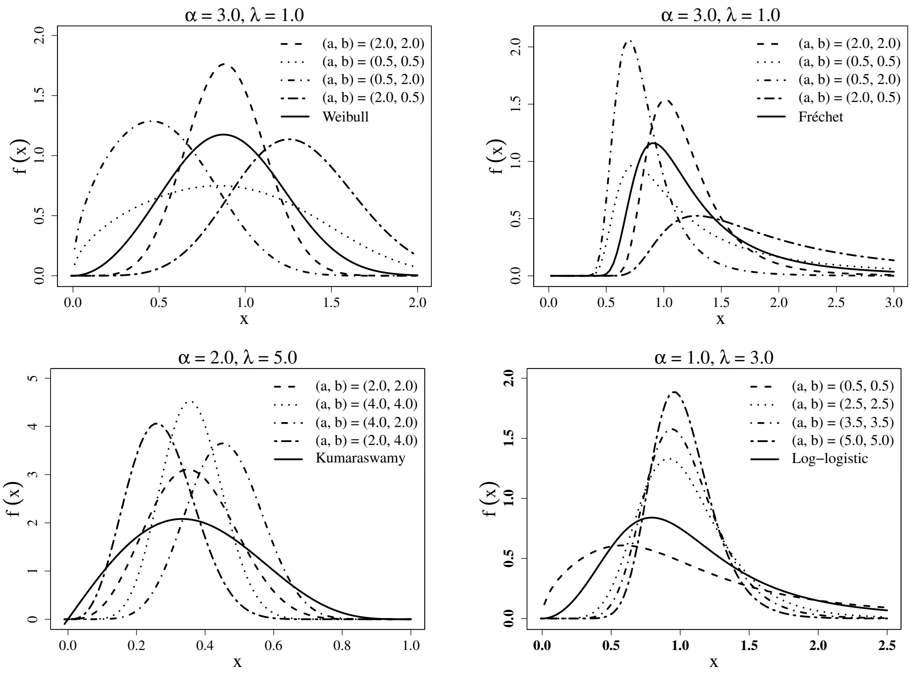

Figure 1. The pdf of the BW, BF, BKw, and BLL distribution, for several values of parameters a, b, α, and λ, respectively.

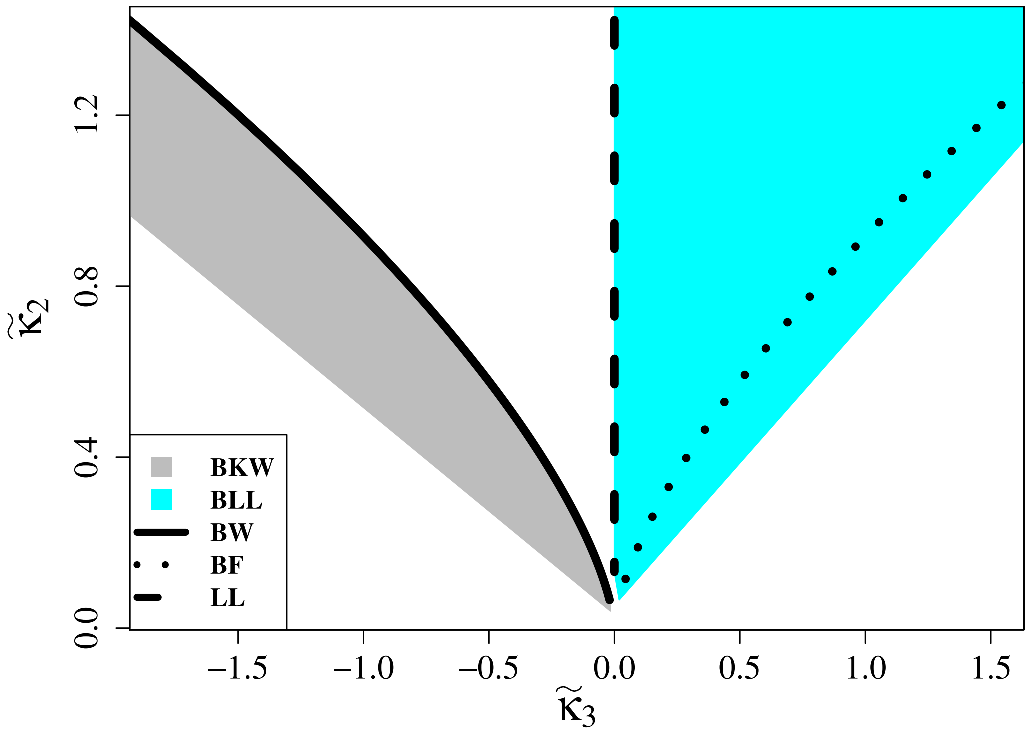

Figure 2. Diagram of the LCs $(\widetilde{\kappa}_3, \widetilde{\kappa}_2)$ for BW, BF, BKw, and BLL models.

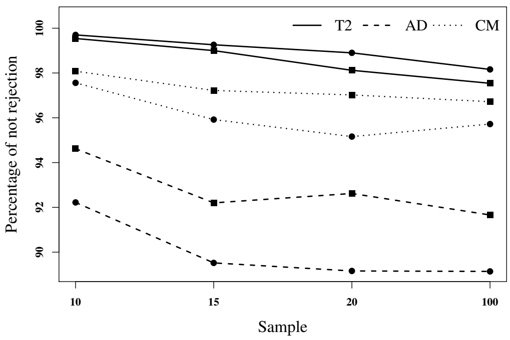

(a) ■ BW($\alpha = 5, \lambda = 1$), ● BW($\alpha = 8, \lambda = 1$)

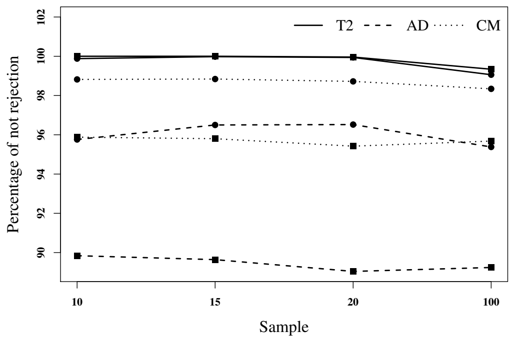

(b) ■ BF($\alpha = 8, \lambda = 1$), ● BF($\alpha = 3, \lambda = 2$)

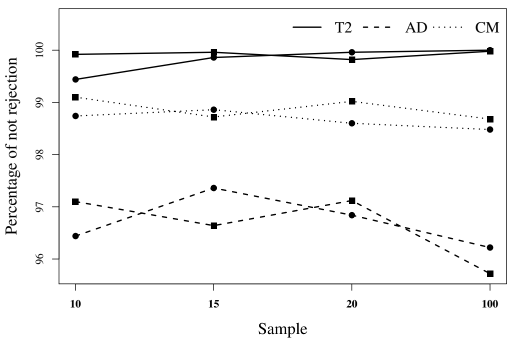

(c) ■ BKW($\alpha = 0.5, \lambda = 8$), ● BKW($\alpha = 1, \lambda = 15$)

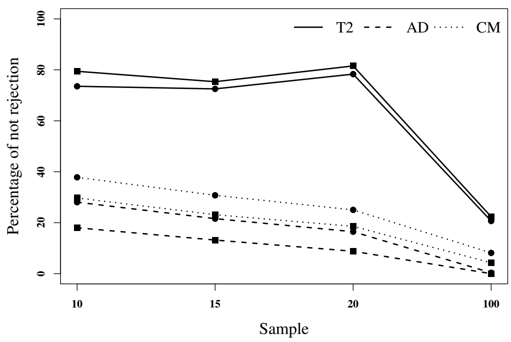

(d) ■ BLL($\alpha = 8, \lambda = 0.6$), ● BLL($\alpha = 8, \lambda = 1$)

Figure 3. The GoF measure of the BW, BF, BKw, and BLL distribution, with $a = 1$ and $b = 1$ parameters.

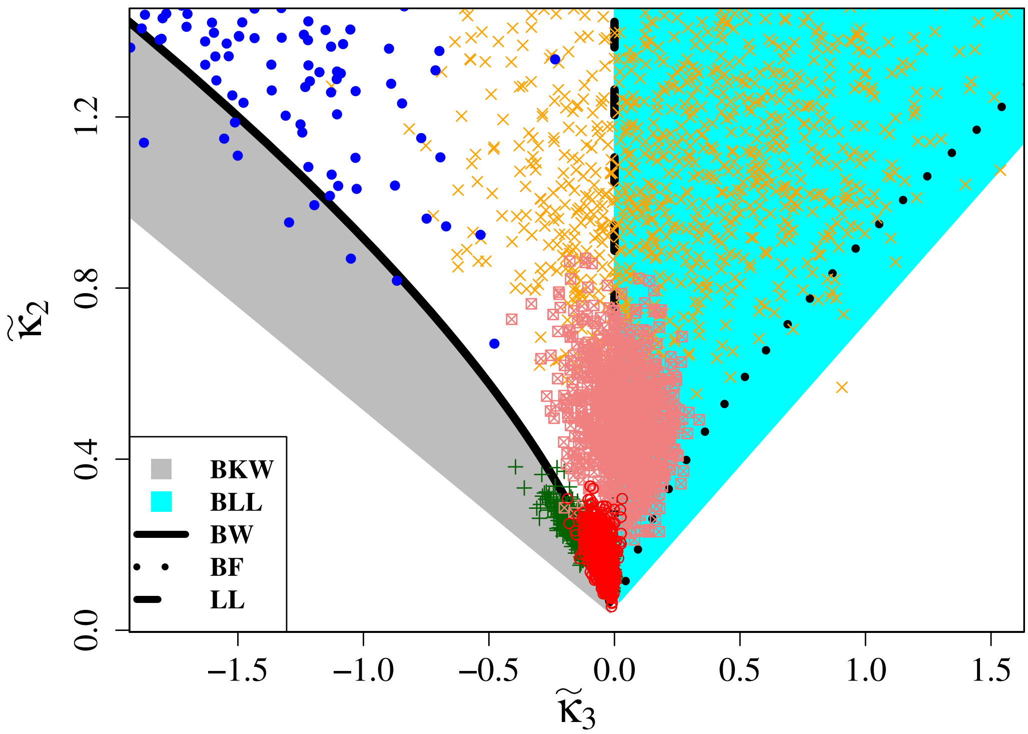

Figure 4. Diagram of the LCs $(\widetilde{\kappa}_3, \widetilde{\kappa}_2)$ showing the manifolds of theoretical LCs for the BKw, BLL, BW, BF, and LL models, as well as a collection of sample LCs representing breaking (+), guinea.pig (⊠), stress-rupture (●), airborne (×), and river flow (○) data sets.

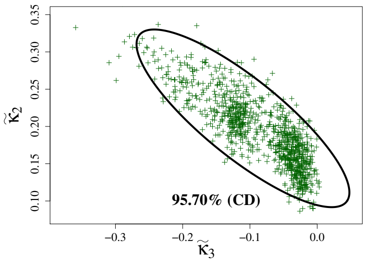

(a) Confidence ellipses-BW

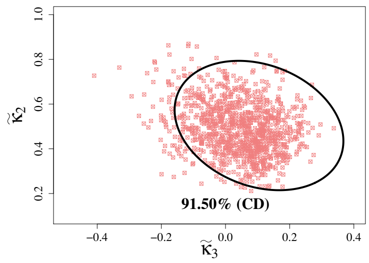

(b) Confidence ellipses-BLL

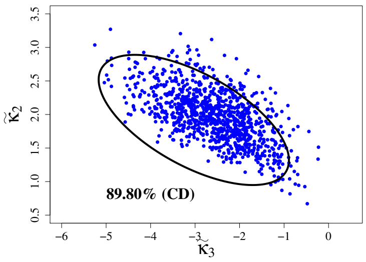

(c) Confidence ellipses-BW

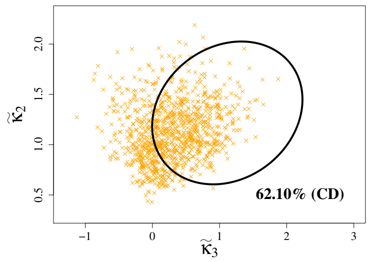

(d) Confidence ellipses-BLL

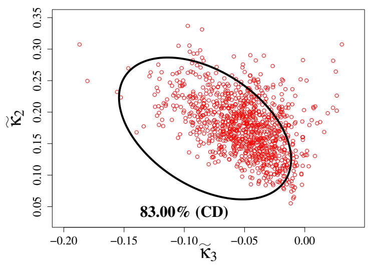

(e) Confidence ellipses-BKw

Figure 5. Confidence ellipses for each data set.

Appendix A. Proof of PWMs for Baseline Distributions

In this appendix, we derive PWM expressions for Fréchet and Kumaraswamy distributions.

A.1. Fréchet PWM

Applying the Fréchet quantile function

$$Q[F(x)] = \lambda\,[-\log(F(x))]^{-{}^{1}/_{\alpha}}$$

to (3), and considering the substitution $u = -\log(F(x))$, we obtain:

$$\mathcal{M}_{l,j,k} = \lambda^l \int_0^\infty u^{-{}^{l}/_{\alpha}}\ \mathrm{e}^{-u(j+1)}\ \left(1-\mathrm{e}^{-u}\right)^k\ \mathrm{d}\,u.$$

Taking into account the following series expansion described in [97,98]

$$(1-z)^j = \sum_{r=0}^{\infty}\binom{j}{r}(-1)^r\, z^r,$$

for $|z| < 1$ and $j > 0$, (**??**) becomes:

$$\mathcal{M}_{l,j,k} = \lambda^l \sum_{r=0}^{\infty}\binom{k}{r}(-1)^r \int_0^\infty u^{-{}^{l}/_{\alpha}}\ \mathrm{e}^{-u(j+r+1)}\ \mathrm{d}\,u.$$

From $\Gamma(\delta) = v^\delta \int_0^\infty x^{\delta-1}\,\mathrm{e}^{-vx}\ \mathrm{d}\,x$, the following result holds:

$$\mathcal{M}_{l,j,k} = \lambda^l\,\Gamma\left(1-\frac{l}{\alpha}\right)\sum_{r=0}^{\infty}\binom{k}{r}(-1)^r\frac{1}{(j+r+1)^{1-{}^{l}/_{\alpha}}},$$

For integer, non-negative values of k, we have [99, p. 612]:

$$\mathcal{M}_{l,j,k} = \lambda^l\,\Gamma\left(1-\frac{l}{\alpha}\right)\sum_{r=0}^{k}\binom{k}{r}(-1)^r\frac{1}{(j+r+1)^{1-{}^{l}/_{\alpha}}}.$$

The last results are valid for $(1 - {}^{l}/_{\alpha}) \notin \mathbb{Z}_-$.

A.2. Kumaraswamy PWM

Applying the Kumaraswamy model quantile function $Q[F(x)] = \left[1-(1-F(x))^{{}^{1}/_{\lambda}}\right]^{{}^{1}/_{\alpha}}$ in (3), and considering the substitution $u = 1-(1-F(x))^{{}^{1}/_{\lambda}}$, we have:

$$\mathcal{M}_{l,j,k} = \lambda\int_0^1 u^{{}^{l}/_{\alpha}}(1-u)^{\lambda(k+1)-1}[1-(1-u)^\lambda]^j\,\mathrm{d}\,u.$$

Again, take $v = (1-u)^\lambda$ and use [99, p. 271]

$$\int_a^b f(x)\,\mathrm{d}\,x = -\int_b^a f(x)\,\mathrm{d}\,x,$$

to obtain

$$\mathcal{M}_{l,j,k} = \int_0^1 (1 - v^{1/\lambda})^{l/\alpha}(1-v)^j v^k \,\mathrm{d}\,v.$$

Invoking (**??**), we have

$$\mathcal{M}_{l,j,k} = \sum_{r=0}^{\infty} \binom{j}{r} (-1)^r \int_0^1 (1 - v^{1/\lambda})^{l/\alpha} v^{r+k} \,\mathrm{d}\,v.$$

Given $t = 1 - v^{1/\lambda}$, we obtain

$$\mathcal{M}_{l,j,k} = \lambda \sum_{r=0}^{\infty} \binom{j}{r} (-1)^r \int_0^1 t^{l/\alpha}(1-t)^{\lambda(k+r+1)-1} \,\mathrm{d}\,t.$$

As $B(\delta, \boldsymbol{\tau}) = \int_0^1 x^{\delta-1}(1-x)^{\tau-1}\,\mathrm{d}\,x$, the following holds:

$$\mathcal{M}_{l,j,k} = \lambda \sum_{r=0}^{\infty} \binom{j}{r} (-1)^r B\left[1 + {}^{l}\!/\!_{\alpha},\, \lambda(k+r+1)\right].$$

For integer, non-negative values of j, we have that [99, p. 612]:

$$\mathcal{M}_{l,j,k} = \lambda \sum_{r=0}^{j} \binom{j}{r} (-1)^r B\left[1 + {}^{l}\!/\!_{\alpha},\, \lambda(k+r+1)\right].$$

Appendix B. Proof of GoF Criteria

In this appendix, we furnish proofs for Propositions 4.1, 4.2, 4.3, and 4.4.

B.1. General Derivation

According to (11), in order to derive the sought statistics for the distribution, we need to obtain the following quantities: (i) the estimates $\widehat{\widehat{\kappa}}_2$ and $\widehat{\widehat{\kappa}}_3$ and (ii) $\widehat{\boldsymbol{K}}^{-1}$.

With the outputs from Algorithm 2 and 3, the sought statistics can be obtained according to the algebraic manipulation implied by (11).

In the next subsections, for each considered model, we state the necessary inputs for the above algorithms and derive the statistics.

Algorithm 2: Computation of $\widehat{\widetilde{\kappa}}_2$ and $\widehat{\widetilde{\kappa}}_3$

Step 1. If BW or BKw models are considered, then let $\boldsymbol{\theta} = \begin{bmatrix}\lambda & \alpha & b\end{bmatrix}^\top$; otherwise $\boldsymbol{\theta} = \begin{bmatrix}\lambda & \alpha & a\end{bmatrix}^\top$;
Step 2. Compute log-likelihood function $\ell(\boldsymbol{\theta})$;
Step 3. Derive the ML estimates $\widehat{\boldsymbol{\theta}}$ by solving the score vector at zero, which can be performed by means of iterative methods, such as the Broyden-Fletcher-Goldfarb-Shanno (BFGS) algorithm;
Step 4. Derive estimates for $\widetilde{\kappa}_2$ and $\widetilde{\kappa}_3$ LCs based on $\widehat{\widetilde{\kappa}}_2 = g_2(\widehat{\boldsymbol{\theta}})$ and $\widehat{\widetilde{\kappa}}_3 = g_3(\widehat{\boldsymbol{\theta}})$.

Algorithm 3: Computation of $\widehat{\boldsymbol{K}}^{-1}$

Step 1. Compute the LC matrix $\widehat{\boldsymbol{J}}$ according to (9), considering the particular functions $g_2(\cdot)$ and $g_3(\cdot)$;
Step 2. Derive the matrix $\boldsymbol{\Sigma}$ according to (10);
Step 3. Compute: $\widehat{\boldsymbol{K}} = \widehat{\boldsymbol{J}}^\top \cdot \widehat{\boldsymbol{\Sigma}} \cdot \widehat{\boldsymbol{J}}$;
Step 4. If $\widehat{\boldsymbol{K}}$ is nonsingular, compute $\widehat{\boldsymbol{K}}^{-1}$ by usual inversion [82] [83]; otherwise compute the generalized inverse of $\widehat{\boldsymbol{K}}$ [84] [85].

B.2. Beta-Weibull Distribution

B.2.1. Log-likelihood Function

$$\ell(\boldsymbol{\theta}) = n\log(\alpha) - n\,\alpha\log(\lambda) - n\log\, B(1,\, b) + (\alpha-1)\sum_{r=1}^{n}\log(x_r) - b\sum_{r=1}^{n}\left(\frac{x_r}{\lambda}\right)^{\alpha}.$$

B.2.2. Score vector components

$$\begin{aligned}
\frac{\partial \ell(\boldsymbol{\theta})}{\partial \alpha} &= \frac{n}{\alpha} + \sum_{r=1}^{n}\log\left(\frac{x_r}{\lambda}\right) - b\sum_{r=1}^{n}\left(\frac{x_r}{\lambda}\right)^{\alpha}\log\left(\frac{x_r}{\lambda}\right),\\
\frac{\partial \ell(\boldsymbol{\theta})}{\partial \lambda} &= -n\frac{\alpha}{\lambda} + b\frac{\alpha}{\lambda^{\alpha+1}}\sum_{r=1}^{n} x_r^{\alpha},\\
\frac{\partial \ell(\boldsymbol{\theta})}{\partial b} &= -n\left\{\psi(b) - \psi(1+b)\right\} - \frac{1}{\lambda^{\alpha}}\sum_{r=1}^{n} x_r^{\alpha}.
\end{aligned}$$

B.2.3. Functions $g_2(\boldsymbol{\theta})$ and $g_3(\boldsymbol{\theta})$

$$g_2(\boldsymbol{\theta}) = \frac{1}{\alpha^2}\psi^{(1)}(1) \quad \text{and} \quad g_3(\boldsymbol{\theta}) = \frac{1}{\alpha^3}\psi^{(2)}(1).$$

B.2.4. Information Matrix and Its Inverse

$$\boldsymbol{H}_{\text{BW}} = -\frac{\partial^2 \ell(\boldsymbol{\theta})}{\partial \boldsymbol{\theta}^\top \partial \boldsymbol{\theta}} = \begin{bmatrix} \text{U}_{\alpha\alpha} & \text{U}_{\alpha\lambda} & \text{U}_{\alpha b} \\ \text{U}_{\lambda\alpha} & \text{U}_{\lambda\lambda} & \text{U}_{\lambda b} \\ \text{U}_{b\alpha} & \text{U}_{b\lambda} & \text{U}_{bb} \end{bmatrix},$$

where $\text{U}_{\alpha\alpha} = \frac{n}{\alpha^2} + b\xi_2^{\text{BW}}$, $\text{U}_{\alpha\lambda} = \text{U}_{\lambda\alpha} = \frac{1}{\lambda}(n - b\xi_3^{\text{BW}})$, $\text{U}_{\alpha b} = \text{U}_{b\alpha} = \xi_1^{\text{BW}}$, $\text{U}_{\lambda\lambda} = [b\alpha(\alpha+1)\xi_0^{\text{BW}} - n\alpha]/\lambda^2$, $\text{U}_{\lambda b} = \text{U}_{b\lambda} = -\frac{\alpha}{\lambda}\xi_0^{\text{BW}}$, $\text{U}_{bb} = n[\psi^{(1)}(b) - \psi^{(1)}(1+b)]$, $\xi_s^{\text{BW}} = \sum_{r=1}^{n} \left(\frac{x_r}{\widehat{\lambda}}\right)^{\widehat{\alpha}} \log^s\left(\frac{x_r}{\widehat{\lambda}}\right)$, for $s = 0, 1, 2$; and $\xi_3^{\text{BW}} = \sum_{r=1}^{n} \left(\frac{x_r}{\lambda}\right)^{\alpha} \left[\log\left(\frac{x_r}{\lambda}\right)^{\alpha} + 1\right]$.

If the determinant $|\boldsymbol{H}_{\text{BW}}| \neq 0$, the asymptotic covariance matrix is given by $\boldsymbol{\Sigma}_{\text{BW}} \approx \boldsymbol{H}_{\text{BW}}^{-1}$, where the usual matrix inversion is applied [82,83]; otherwise we apply the generalized Moore-Penrose inverse [84,85].

B.2.5. Log-cumulant Matrix

$$\boldsymbol{J}_{\text{BW}} = -\begin{bmatrix} \frac{2}{\alpha^3}\psi^{(1)}(1) & \frac{3}{\alpha^4}\psi^{(2)}(1) \\ 0 & 0 \\ 0 & 0 \end{bmatrix}.$$

B.2.6. Asymptotic Covariance Matrix and Its Inverse

$$\boldsymbol{K}_{\text{BW}} = \left(\frac{\text{U}_{\alpha\alpha}\text{U}_{bb} - \text{U}_{\lambda b}^2}{\alpha^8 |\boldsymbol{H}_{\text{BW}}|}\right) \cdot \begin{bmatrix} 4\alpha^2\psi^{(1)}(1)^2 & 6\alpha\psi^{(1)}(1)\psi^{(2)}(1) \\ 6\alpha\psi^{(1)}(1)\psi^{(2)}(1) & 9\psi^{(2)}(1)^2 \end{bmatrix}.$$

where

$$|\boldsymbol{H}_{\text{BW}}| = \text{U}_{\alpha\alpha}(\text{U}_{\lambda\lambda}\text{U}_{bb} - \text{U}_{\lambda b}^2) + \text{U}_{\alpha\lambda}(\text{U}_{\alpha b}\text{U}_{\lambda b} - \text{U}_{\alpha\lambda}\text{U}_{bb}) + \text{U}_{\alpha b}(\text{U}_{\alpha\lambda}\text{U}_{\lambda b} - \text{U}_{\alpha b}\text{U}_{\lambda\lambda}).$$

Because $\boldsymbol{K}_{\text{BW}}$ is singular, the generalized Moore-Penrose inverse was computed [84, p. 508]:

$$\boldsymbol{K}_{\text{BW}}^{-1} = \left(\frac{\alpha^6 |\boldsymbol{H}_{\text{BW}}|}{\text{U}_{\alpha\alpha}\text{U}_{bb} - \text{U}_{\lambda b}^2}\right) \begin{bmatrix} (2\psi^{(1)}(1))^{-2} & 0 \\ 0 & 0 \end{bmatrix}.$$

B.2.7. Hotelling's T^2 statistic Derivation

Therefore, we obtain:

$$T_{\text{BW}}^2 = \frac{n\widehat{\alpha}^6}{4}\left(\frac{1}{\widehat{\alpha}^2} - \frac{1}{\alpha^2}\right)^2 \left(\frac{|\widehat{\boldsymbol{H}}_{\text{BW}}|}{\text{U}_{\widehat{\alpha}\widehat{\alpha}}\text{U}_{\widehat{b}\widehat{b}} - \text{U}_{\widehat{\lambda}\widehat{b}}^2}\right).$$

B.3. Beta-Fréchet Distribution

B.3.1. Log-likelihood Function

$$\ell(\boldsymbol{\theta}) = n\log(\alpha) + n\,\alpha\log(\lambda) - n\log\,B(a,\,1) - (1+\alpha)\sum_{r=1}^{n}\log(x_r) - a\sum_{r=1}^{n}\left(\frac{\lambda}{x_r}\right)^{\alpha}.$$

B.3.2. Score vector components

$$\frac{\partial\ell(\boldsymbol{\theta})}{\partial\alpha} = \frac{n}{\alpha} + n\log(\lambda) - \sum_{r=1}^{n}\log\left(x_r\right) - a\sum_{r=1}^{n}\left(\frac{\lambda}{x_r}\right)^{\alpha}\log\left(\frac{\lambda}{x_r}\right),$$
$$\frac{\partial\ell(\boldsymbol{\theta})}{\partial\lambda} = n\frac{\alpha}{\lambda} - a\,\alpha\,\lambda^{\alpha-1}\sum_{r=1}^{n}x_r^{-\alpha},$$
$$\frac{\partial\ell(\boldsymbol{\theta})}{\partial a} = -n\left\{\psi(a) - \psi(1+a)\right\} - \lambda^{\alpha}\sum_{r=1}^{n}x_r^{-\alpha}.$$

B.3.3. Functions $g_2(\boldsymbol{\theta})$ and $g_3(\boldsymbol{\theta})$

$$g_2(\boldsymbol{\theta}) = \frac{1}{\alpha^2}\psi^{(1)}(1) \quad\text{and}\quad g_3(\boldsymbol{\theta}) = -\frac{1}{\alpha^3}\psi^{(2)}(1).$$

B.3.4. Information Matrix and Its Inverse

$$\boldsymbol{H}_{\text{BF}} = -\frac{\partial^2\ell(\boldsymbol{\theta})}{\partial\boldsymbol{\theta}^{\top}\partial\boldsymbol{\theta}} = \begin{bmatrix} \mathrm{U}_{\alpha\alpha} & \mathrm{U}_{\alpha\lambda} & \mathrm{U}_{\alpha a} \\ \mathrm{U}_{\lambda\alpha} & \mathrm{U}_{\lambda\lambda} & \mathrm{U}_{\lambda a} \\ \mathrm{U}_{a\alpha} & \mathrm{U}_{a\lambda} & \mathrm{U}_{aa} \end{bmatrix},$$

where $\mathrm{U}_{\alpha\alpha} = \frac{n}{\alpha^2} + a\xi_2^{\text{BF}}$, $\mathrm{U}_{\alpha\lambda} = \mathrm{U}_{\lambda\alpha} = \frac{1}{\lambda}(a\xi_3^{\text{BF}} - n)$, $\mathrm{U}_{\alpha a} = \mathrm{U}_{a\alpha} = \xi_1^{\text{BF}}$, $\mathrm{U}_{\lambda\lambda} = \frac{1}{\lambda^2}\left[n\alpha - a\alpha(1-\alpha)\xi_0^{\text{BF}}\right]$, $\mathrm{U}_{\lambda a} = \mathrm{U}_{a\lambda} = \frac{\alpha}{\lambda}\xi_0^{\text{BF}}$, $\mathrm{U}_{aa} = n[\psi^{(1)}(a) - \psi^{(1)}(1+a)]$, $\xi_s^{\text{BF}} = \sum_{r=1}^{n}\left(\frac{\widehat{\lambda}}{x_r}\right)^{\widehat{\alpha}}\log^s\left(\frac{\widehat{\lambda}}{x_r}\right)$ with $s = 0, 1, 2$, and $\xi_3^{\text{BF}} = \sum_{r=1}^{n}\left(\frac{\lambda}{x_r}\right)^{\alpha}\left[\log(\frac{\lambda}{x_r})^{\alpha} + 1\right]$.

If the determinant $|\boldsymbol{H}_{\text{BF}}| \neq 0$, the asymptotic covariance matrix is given by $\boldsymbol{\Sigma}_{\text{BF}} \approx \boldsymbol{H}_{\text{BF}}^{-1}$ [82,83]; otherwise we apply the generalized Moore-Penrose inverse [84,85].

B.3.5. Log-cumulant Matrix

$$\boldsymbol{J}_{\mathrm{BF}} = \begin{bmatrix} -\frac{2}{\alpha^3}\psi^{(1)}(1) & \frac{3}{\alpha^4}\psi^{(2)}(1) \\ 0 & 0 \\ 0 & 0 \end{bmatrix}.$$

B.3.6. Asymptotic Covariance Matrix and Its Inverse

$$\boldsymbol{K}_{\mathrm{BF}} = \left(\frac{\mathrm{U}_{\alpha\alpha}\mathrm{U}_{aa} - \mathrm{U}_{\lambda a}^2}{\alpha^8|\boldsymbol{H}_{\mathrm{BF}}|}\right) \cdot \begin{bmatrix} 4\widehat{\alpha}^2\psi^{(1)}(1)^2 & -6\widehat{\alpha}\psi^{(1)}(1)\psi^{(2)}(1) \\ -6\widehat{\alpha}\psi^{(1)}(1)\psi^{(2)}(1) & 9\psi^{(2)}(1)^2 \end{bmatrix}.$$

Because $\boldsymbol{K}_{\mathrm{BF}}$ is singular, the generalized Moore-Penrose inverse was computed [84, p. 508]:

$$\boldsymbol{K}_{\mathrm{BF}}^{-1} = \left(\frac{\alpha^6|\boldsymbol{H}_{\mathrm{BF}}|}{\mathrm{U}_{\alpha\alpha}\mathrm{U}_{aa} - \mathrm{U}_{\lambda a}^2}\right) \begin{bmatrix} \left(2\psi^{(1)}(1)\right)^{-2} & 0 \\ 0 & 0 \end{bmatrix}.$$

B.3.7. Hotelling's T^2 statistic Derivation

Therefore, we obtain:

$$T_{\mathrm{BF}}^2 = \frac{n\widehat{\alpha}^6}{4}\left(\frac{1}{\widehat{\alpha}^2} - \frac{1}{\alpha^2}\right)^2 \left(\frac{|\widehat{\boldsymbol{H}}_{\mathrm{BF}}|}{\mathrm{U}_{\widehat{\alpha}\widehat{\alpha}}\mathrm{U}_{\widehat{a}\widehat{a}} - \mathrm{U}_{\widehat{\lambda}\widehat{a}}^2}\right).$$

B.4. Beta-Kumaraswamy Distribution

B.4.1. Log-likelihood Function

$$\ell(\boldsymbol{\theta}) = n\log(\alpha\,\lambda) - n\log\,B(1,\,b) + (\alpha-1)\sum_{r=1}^{n}\log(x_r) + (\lambda\,b-1)\sum_{r=1}^{n}\log\left(1-x_r^{\alpha}\right).$$

B.4.2. Score vector components

$$
\begin{aligned}
\frac{\partial \ell(\boldsymbol{\theta})}{\partial \alpha} &= \frac{n}{\alpha} + \sum_{i=1}^{n} \log\left(x_r\right) - (\lambda b - 1) \sum_{r=1}^{n} \frac{x_r^{\alpha} \log(x_r)}{1 - x_r^{\alpha}}, \\
\frac{\partial \ell(\boldsymbol{\theta})}{\partial \lambda} &= \frac{n}{\lambda} + b \sum_{r=1}^{n} \log(1 - x_r^{\alpha}), \\
\frac{\partial \ell(\boldsymbol{\theta})}{\partial b} &= -n\left\{\psi(b) - \psi(1+b)\right\} + \lambda \sum_{r=1}^{n} \log(1 - x_r^{\alpha}).
\end{aligned}
$$

B.4.3. Functions $g_2(\boldsymbol{\theta})$ and $g_3(\boldsymbol{\theta})$

$$
g_2(\boldsymbol{\theta}) = \frac{\psi^{(1)}(1) - \psi^{(1)}(\lambda b + 1)}{\alpha^2} \quad \text{and} \quad g_3(\boldsymbol{\theta}) = \frac{\psi^{(2)}(1) - \psi^{(2)}(\lambda b + 1)}{\alpha^3}.
$$

B.4.4. Information Matrix and Its inverse

$$
\boldsymbol{H}_{\text{BKw}} = -\frac{\partial^2 \ell(\boldsymbol{\theta})}{\partial \boldsymbol{\theta}^{\top} \partial \boldsymbol{\theta}} = \begin{bmatrix} \mathrm{U}_{\alpha\alpha} & \mathrm{U}_{\alpha\lambda} & \mathrm{U}_{\alpha b} \\ \mathrm{U}_{\lambda\alpha} & \mathrm{U}_{\lambda\lambda} & \mathrm{U}_{\lambda b} \\ \mathrm{U}_{b\alpha} & \mathrm{U}_{b\lambda} & \mathrm{U}_{bb} \end{bmatrix},
$$

where $\mathrm{U}_{\alpha\alpha} = \frac{n}{\alpha^2} + (\lambda b - 1)\sum_{r=1}^{n} \frac{x_r^{\alpha} \log^2(x_r)}{(1-x_r^{\alpha})^2}$, $\mathrm{U}_{\alpha\lambda} = \mathrm{U}_{\lambda\alpha} = b\sum_{r=1}^{n} \frac{x_r^{\alpha} \log(x_r)}{(1-x_r^{\alpha})}$, $\mathrm{U}_{\alpha b} = \mathrm{U}_{b\alpha} = \lambda\sum_{r=1}^{n} \frac{x_r^{\alpha} \log(x_r)}{(1-x_r^{\alpha})}$, $\mathrm{U}_{\lambda\lambda} = \frac{n}{\lambda^2}$, $\mathrm{U}_{\lambda b} = \mathrm{U}_{b\lambda} = -\sum_{r=1}^{n} \log(1 - x_r^{\alpha})$, and $\mathrm{U}_{bb} = n[\psi^{(1)}(b) - \psi^{(1)}(1+b)]$.

If the determinant $|\boldsymbol{H}_{\text{BKw}}| \neq 0$, the asymptotic covariance matrix is given by

$$
\boldsymbol{\Sigma}_{\text{BKw}} \approx \frac{1}{|\boldsymbol{H}_{\text{BKw}}|} \begin{bmatrix} \mathrm{U}^{b}_{\alpha\alpha} & \mathrm{U}^{b}_{\alpha\lambda} & \mathrm{U}^{b}_{\alpha b} \\ \mathrm{U}^{b}_{\lambda\alpha} & \mathrm{U}^{b}_{\lambda\lambda} & \mathrm{U}^{b}_{\lambda b} \\ \mathrm{U}^{b}_{b\alpha} & \mathrm{U}^{b}_{b\lambda} & \mathrm{U}^{b}_{bb} \end{bmatrix},
$$

with $\mathrm{U}^{b}_{\alpha\alpha} = \mathrm{U}_{\lambda\lambda}\mathrm{U}_{bb} - \mathrm{U}^2_{\lambda b}$, $\mathrm{U}^{b}_{\alpha\lambda} = \mathrm{U}^{b}_{\lambda\alpha} = \mathrm{U}_{\alpha b}\mathrm{U}_{\lambda b} - \mathrm{U}_{\alpha b}\mathrm{U}_{\lambda\lambda}$, $\mathrm{U}^{b}_{\alpha b} = \mathrm{U}^{b}_{b\alpha} = \mathrm{U}_{\alpha\lambda}\mathrm{U}_{\lambda b} - \mathrm{U}_{\alpha b}\mathrm{U}_{\lambda\lambda}$, $\mathrm{U}^{b}_{\lambda\lambda} = \mathrm{U}_{\alpha\alpha}\mathrm{U}_{bb} - \mathrm{U}^2_{\alpha b}$, $\mathrm{U}^{b}_{\lambda b} = \mathrm{U}^{b}_{b\lambda} = \mathrm{U}_{\alpha\lambda}\mathrm{U}_{\alpha b} - \mathrm{U}_{\alpha\alpha}\mathrm{U}_{\lambda b}$, $\mathrm{U}^{b}_{bb} = \mathrm{U}_{\alpha\alpha}\mathrm{U}_{\lambda\lambda} - \mathrm{U}^2_{\alpha\lambda}$; otherwise we apply the generalized Moore-Penrose inverse [84,85].

B.4.5. Log-cumulant Matrix

$$\boldsymbol{J}_{\text{BKw}} = \begin{bmatrix} J_{12} & J_{13} \\ J_{22} & J_{23} \\ J_{32} & J_{33} \end{bmatrix},$$

where

$$\begin{aligned}
J_{12} &= \frac{2}{\alpha^3}\{\psi^{(1)}(\lambda b+1) - \psi^{(1)}(1)\}, \\
J_{13} &= \frac{3}{\alpha^4}\{\psi^{(2)}(\lambda b+1) - \psi^{(2)}(1)\}, \\
J_{22} &= \frac{b}{\alpha^2}\psi^{(2)}(\lambda b+1), \quad J_{23} = \frac{b}{\alpha^3}\psi^{(3)}(\lambda b+1), \\
J_{32} &= \frac{\lambda}{\alpha^2}\psi^{(2)}(\lambda b+1), \quad J_{33} = \frac{\lambda}{\alpha^3}\psi^{(3)}(\lambda b+1).
\end{aligned}$$

B.4.6. Asymptotic Covariance Matrix and Its Inverse

$$\boldsymbol{K}_{\text{BKw}} = \frac{1}{|\boldsymbol{H}_{\text{BKw}}|}\begin{bmatrix} \delta_{22} & \delta_{32} \\ \delta_{23} & \delta_{33} \end{bmatrix},$$

where

$$\begin{aligned}
\delta_{22} &= J_{12}(J_{12}\mathrm{U}^b_{\alpha\alpha} + J_{22}\mathrm{U}^b_{\lambda\alpha} + J_{32}\mathrm{U}^b_{b\alpha}) + J_{22}(J_{12}\mathrm{U}^b_{\alpha\lambda} + J_{22}\mathrm{U}^b_{\lambda\lambda} + J_{32}\mathrm{U}^b_{b\lambda}) \\
&\quad + J_{32}(J_{12}\mathrm{U}^b_{\alpha b} + J_{22}\mathrm{U}^b_{\lambda b} + J_{32}\mathrm{U}^b_{bb}), \\
\delta_{23} = \delta_{32} &= J_{13}(J_{12}\mathrm{U}^b_{\alpha\alpha} + J_{22}\mathrm{U}^b_{\lambda\alpha} + J_{32}\mathrm{U}^b_{b\alpha}) + J_{23}(J_{12}\mathrm{U}^b_{\alpha\lambda} + J_{22}\mathrm{U}^b_{\lambda\lambda} + J_{32}\mathrm{U}^b_{b\lambda}) \\
&\quad + J_{33}(J_{12}\mathrm{U}^b_{\alpha b} + J_{22}\mathrm{U}^b_{\lambda b} + J_{32}\mathrm{U}^b_{bb}), \\
\delta_{33} &= J_{13}(J_{13}\mathrm{U}^b_{\alpha\alpha} + J_{23}\mathrm{U}^b_{\lambda\alpha} + J_{33}\mathrm{U}^b_{b\alpha}) + J_{23}(J_{13}\mathrm{U}^b_{\alpha\lambda} + J_{23}\mathrm{U}^b_{\lambda\lambda} + J_{33}\mathrm{U}^b_{b\lambda}) \\
&\quad + J_{33}(J_{13}\mathrm{U}^b_{\alpha b} + J_{23}\mathrm{U}^b_{\lambda b} + J_{33}\mathrm{U}^b_{bb}).
\end{aligned}$$

If $\delta_{22}\delta_{33} > \delta_{23}^2$ and $|\boldsymbol{H}_{\text{BKw}}| \neq 0$, then the inverse is given by

$$\boldsymbol{K}^{-1}_{\text{BKw}} = \frac{|\boldsymbol{H}_{\text{BKw}}|}{\delta_{22}\delta_{33} - \delta_{23}^2}\begin{bmatrix} \delta_{33} & -\delta_{32} \\ -\delta_{23} & \delta_{22} \end{bmatrix},$$

otherwise we apply the generalized Moore-Penrose inverse [84,85].

B.4.7. Hotelling's T^2 statistic Derivation

The sought T^2_{BKw} statistic is:

$$T^2_{\text{BKw}} = \frac{n|\widehat{\boldsymbol{H}}_{\text{BKw}}|}{\widehat{\delta}_{22}\widehat{\delta}_{33} - \widehat{\delta}_{23}^2}\left[\widehat{\delta}_{33}\left(\widehat{\widetilde{\kappa}}_2 - \widetilde{\kappa}_2\right)^2 + \widehat{\delta}_{22}\left(\widehat{\widetilde{\kappa}}_3 - \widetilde{\kappa}_3\right)^2 - 2\widehat{\delta}_{23}\left(\widehat{\widetilde{\kappa}}_2 - \widetilde{\kappa}_2\right)\left(\widehat{\widetilde{\kappa}}_3 - \widetilde{\kappa}_3\right)\right].$$

B.5. Beta-log-logistic Distribution

B.5.1. Log-likelihood Function

$$\ell(\boldsymbol{\theta}) = n\log\left(\frac{\lambda}{\alpha}\right) - n\log\, B(a,\,1) + (a\lambda - 1)\sum_{r=1}^{n}\log\left(\frac{x_r}{\alpha}\right) - (a+1)\sum_{r=1}^{n}\log\left[1 + (x_r/\alpha)^{\lambda}\right].$$

B.5.2. Score vector components

$$\begin{aligned}
\frac{\partial\ell(\boldsymbol{\theta})}{\partial\alpha} &= -\frac{n\lambda\, a}{\alpha} + \frac{\lambda(a+1)}{\alpha}\sum_{r=1}^{n}\frac{(x_r/\alpha)^{\lambda}}{\left[1 + (x_r/\alpha)^{\lambda}\right]},\\
\frac{\partial\ell(\boldsymbol{\theta})}{\partial\lambda} &= \frac{n}{\lambda} + a\sum_{r=1}^{n}\log\left(\frac{x_r}{\alpha}\right) - (a+1)\sum_{r=1}^{n}\frac{(x_r/\alpha)^{\lambda}\log(x_r/\alpha)}{\left[1 + (x_r/\alpha)^{\lambda}\right]},\\
\frac{\partial\ell(\boldsymbol{\theta})}{\partial a} &= -n\left\{\psi(a) - \psi(1+a)\right\} + \lambda\sum_{r=1}^{n}\log\left(\frac{x_r}{\alpha}\right) - \sum_{r=1}^{n}\log\left[1 + (x_r/\alpha)^{\lambda}\right].
\end{aligned}$$

B.5.3. Functions $g_2(\boldsymbol{\theta})$ and $g_3(\boldsymbol{\theta})$

$$g_2(\boldsymbol{\theta}) = \frac{\psi^{(1)}(1) + \psi^{(1)}(1)}{\lambda^2} \quad \text{and} \quad g_3(\boldsymbol{\theta}) = \frac{\psi^{(2)}(1) - \psi^{(2)}(1)}{\lambda^3}.$$

B.5.4. Information Matrix and Its inverse

$$\boldsymbol{H}_{\text{BLL}} = -\frac{\partial^2\ell(\boldsymbol{\theta})}{\partial\boldsymbol{\theta}^{\top}\partial\boldsymbol{\theta}} = \begin{bmatrix} \mathrm{U}_{\alpha\alpha} & \mathrm{U}_{\alpha\lambda} & \mathrm{U}_{\alpha a}\\ \mathrm{U}_{\lambda\alpha} & \mathrm{U}_{\lambda\lambda} & \mathrm{U}_{\lambda a}\\ \mathrm{U}_{a\alpha} & \mathrm{U}_{a\lambda} & \mathrm{U}_{aa}\end{bmatrix},$$

where

$$
\begin{aligned}
\mathrm{U}_{\alpha\alpha} &= -\frac{\lambda}{\alpha^2}\left\{na-(a+1)\sum_{r=1}^{n} z_r\left[1+\frac{\lambda}{1+y_r^{\lambda}}\right]\right\},\\
\mathrm{U}_{\alpha\lambda} &= \frac{1}{\alpha}\left[na-(a+1)\sum_{r=1}^{n}\Big(z_r+\lambda y_r^{\lambda}\log(y_r)\Big)\right],\\
\mathrm{U}_{\alpha a} &= -\frac{\lambda}{\alpha}\sum_{r=1}^{n}(z_r-1),\\
\mathrm{U}_{\lambda\lambda} &= \frac{n}{\lambda^2}+(a+1)\sum_{r=1}^{n}\frac{z_r\log y_r}{1+y_r^{\lambda}}\left[(1+y_r^{\lambda})\log y_r+\frac{\lambda}{\alpha}y_r^{\lambda}\right],\\
\mathrm{U}_{\lambda a} &= -\sum_{r=1}^{n}(1-z_r)\log y_r,\\
\mathrm{U}_{aa} &= n[\psi^{(1)}(a)-\psi^{(1)}(1+a)].
\end{aligned}
$$

with $z_r = y_r^{\lambda}/(1+y_r^{\lambda})$, and $y_r = x_r/\alpha$.

If the determinant $|\boldsymbol{H}_{\mathrm{BLL}}| \neq 0$, the asymptotic covariance matrix is given by

$$
\boldsymbol{\Sigma}_{\mathrm{BLL}} \approx \frac{1}{|\boldsymbol{H}_{\mathrm{BLL}}|}\begin{bmatrix}\mathrm{U}^a_{\alpha\alpha} & \mathrm{U}^a_{\alpha\lambda} & \mathrm{U}^a_{\alpha a}\\ \mathrm{U}^a_{\lambda\alpha} & \mathrm{U}^a_{\lambda\lambda} & \mathrm{U}^a_{\lambda a}\\ \mathrm{U}^a_{a\alpha} & \mathrm{U}^a_{a\lambda} & \mathrm{U}^a_{aa}\end{bmatrix},
$$

with $\mathrm{U}^a_{\alpha\alpha} = \mathrm{U}_{\lambda\lambda}\mathrm{U}_{aa} - \mathrm{U}^2_{\lambda a}$, $\mathrm{U}^a_{\alpha\lambda} = \mathrm{U}^a_{\lambda\alpha} = \mathrm{U}_{\alpha a}\mathrm{U}_{\lambda a} - \mathrm{U}_{\alpha a}\mathrm{U}_{\lambda\lambda}$, $\mathrm{U}^a_{\alpha a} = \mathrm{U}^a_{a\alpha} = \mathrm{U}_{\alpha\lambda}\mathrm{U}_{\lambda a} - \mathrm{U}_{\alpha a}\mathrm{U}_{\lambda\lambda}$, $\mathrm{U}^a_{\lambda\lambda} = \mathrm{U}_{\alpha\alpha}\mathrm{U}_{aa} - \mathrm{U}^2_{\alpha a}$, $\mathrm{U}^a_{\lambda a} = \mathrm{U}^a_{a\lambda} = \mathrm{U}_{\alpha\lambda}\mathrm{U}_{\alpha a} - \mathrm{U}_{\alpha\alpha}\mathrm{U}_{\lambda a}$, $\mathrm{U}^a_{aa} = \mathrm{U}_{\alpha\alpha}\mathrm{U}_{\lambda\lambda} - \mathrm{U}^2_{\alpha\lambda}$; otherwise we apply the generalized Moore-Penrose inverse [84,85].

B.5.5. Log-cumulant Matrix

$$
\boldsymbol{J}_{\mathrm{BLL}} = \begin{bmatrix} J_{12} & J_{13}\\ J_{22} & J_{23}\\ J_{32} & J_{33}\end{bmatrix},
$$

where

$$
\begin{aligned}
J_{12} &= J_{13} = 0, J_{22} = -\frac{2}{\lambda^3}\{\psi^{(1)}(a)+\psi^{(1)}(1)\},\\
J_{23} &= -\frac{3}{\lambda^4}\{\psi^{(2)}(a)-\psi^{(2)}(1)\},\\
J_{32} &= \frac{1}{\lambda^2}\psi^{(2)}(a), J_{33} = \frac{1}{\lambda^3}\psi^{(3)}(a).
\end{aligned}
$$

B.5.6. Asymptotic Covariance Matrix and Its Inverse

$$\boldsymbol{K}_{\mathrm{BLL}} = \frac{1}{|\boldsymbol{H}_{\mathrm{BLL}}|} \begin{bmatrix} \delta_{22} & \delta_{32} \\ \delta_{23} & \delta_{33} \end{bmatrix},$$

where

$$\begin{aligned} \delta_{22} &= J_{22}(J_{22}\mathrm{U}^{a}_{\lambda\lambda} + J_{32}\mathrm{U}^{a}_{a\lambda}) + J_{32}(J_{22}\mathrm{U}^{a}_{\lambda a} + J_{32}\mathrm{U}^{a}_{aa}), \\ \delta_{23} = \delta_{32} &= J_{23}(J_{22}\mathrm{U}^{a}_{\lambda\lambda} + J_{32}\mathrm{U}^{a}_{a\lambda}) + J_{33}(J_{22}\mathrm{U}^{a}_{\lambda a} + J_{32}\mathrm{U}^{a}_{aa}), \\ \delta_{33} &= J_{23}(J_{23}\mathrm{U}^{a}_{\lambda\lambda} + J_{33}\mathrm{U}^{a}_{a\lambda}) + J_{33}(J_{23}\mathrm{U}^{a}_{\lambda a} + J_{33}\mathrm{U}^{a}_{aa}). \end{aligned}$$

If $\delta_{22}\delta_{33} > \delta_{23}^2$ and $|\boldsymbol{H}_{\mathrm{BLL}}| \neq 0$, then the inverse is given by

$$\boldsymbol{K}^{-1}_{\mathrm{BLL}} = \frac{|\boldsymbol{H}_{\mathrm{BLL}}|}{\delta_{22}\delta_{33} - \delta_{23}^2} \begin{bmatrix} \delta_{33} & -\delta_{32} \\ -\delta_{23} & \delta_{22} \end{bmatrix},$$

otherwise we apply the generalized Moore-Penrose inverse [84,85].

B.5.7. Hotelling's T^2 statistic Derivation

The sought T^2_{BLL} statistic is:

$$T^2_{\mathrm{BLL}} = \frac{n|\widehat{\boldsymbol{H}}_{\mathrm{BLL}}|}{\widehat{\delta}_{22}\widehat{\delta}_{33} - \widehat{\delta}_{23}^2} \left[\widehat{\delta}_{33} \left(\widehat{\widetilde{\kappa}}_2 - \widetilde{\kappa}_2 \right)^2 + \widehat{\delta}_{22} \left(\widehat{\widetilde{\kappa}}_3 - \widetilde{\kappa}_3 \right)^2 - 2\widehat{\delta}_{23} \left(\widehat{\widetilde{\kappa}}_2 - \widetilde{\kappa}_2 \right) \left(\widehat{\widetilde{\kappa}}_3 - \widetilde{\kappa}_3 \right) \right].$$